Manufacturing Rev. **6**, 25 (2019)

https://doi.org/10.1051/mfreview/2019023

Manufacturing Review
Available online at:
https://mfr.edp-open.org

REVIEW OPEN ACCESS

A comparative review on cold gas dynamic spraying processes and technologies

Sunday Temitope Oyinbo* and Tien-Chien Jen

Department of Mechanical Engineering Science, University of Johannesburg, Gauteng 2006, South Africa

Received: 16 August 2019 / Accepted: 23 September 2019

Abstract. Cold gas dynamic spraying (CGDS) is a relatively new technology of cold spraying techniques that uses converging-diverging (De Laval) nozzle at a supersonic velocity to accelerate different solid powders towards a substrate where it plastically deforms on the substrate. This deformation results in adhesion to the surface. Several materials with viable deposition capability have been processed through cold spraying, including metals, ceramics, composite materials, and polymers, thereby creating a wide range of opportunities towards harnessing various properties. CGDS is one of the innovative cold spraying processes with fast-growing scientific interests and industrial applications in the field of aerospace, automotive and biotechnology, over the past years. Cold gas spraying with a wide range of materials offers corrosion protection and results in increases in mechanical durability and wear resistance. It creates components with different thermal and electrical conductivities than that substrates would yield, or produces coatings on the substrate components as thermal insulators and high fatigue-strength coatings, and for clearance control, restoration and repairing, or prostheses with improved wear, and produces components with attractive appearances. This review extensively exploits the latest developments in the experimental analysis of CGDS processes. Cold gas dynamic spraying system, coating formation and deposit development, description of process parameter and principles, are summarized. Industrial applications and prospectives of CGDS in future research are also commented.

Keywords: Cold gas dynamic spraying / spraying parameters / deformatiom mechanism / CGDS applications

1 Introduction

Cold gas dynamic spraying (CGDS), is one of the embracing powder deposition spraying processes. This technology was introduced in Russia by the institute for theoretical and applied Mechanics in 1980s [1]. They discovered experimentally that the cold gas spraying process could be termed 'additive manufacturing' techniques. Before this time, Thurston patented on August 12, 1902, a method for gas under high pressure at a velocity of 300 m/s to accelerate metallic powder and subsequently, the deposit was achieved by a high-speed collision on the base material. Major innovative development began In the 1950s by Rochevill, using a gas flow at a velocity higher than those obtained with the existing methods at that time. The flow of gas through a nozzle called the De Laval Nozzle produces a uniform thin coating [1–3].

Several materials like metals, metallic alloys, composite materials and polymer were successfully deposited onto a substrate material by the Russians, and they attained a very high coating deposition rate by the cold gas process. The number of industrial applications for cold spraying has been growing worldwide in the field of aerospace, energy, automobile, biotechnology and military. CGDS is a cold spraying technique for obtaining solid-state surface coating. The deposition during CGDS can be summarised into the molecular attraction between the surface deposit of the particles and the substrates and in-built deposit growth. A high speed ranging from 500 to 1500 ms^{-1} [4] carrier gas accelerates finely divided powder particles (1–50 μm) through converging-diverging De Laval Nozzle. At a supersonic velocity, particles impact and plastically deform on the substrate. The deformation process results in adhesion to the surface [5–10].

Studying of relevant literature has shown that CGDS provides the deposition dynamics that could not be achieved literally by conventional spraying techniques such as plasma spray, wire arc, high-velocity oxy-fuel (HVOF) and wire flame which associate with phase properties changes and high temperatures. These associated limitations can easily be overcome by newly developed technology namely cold spraying coating technology [1,11–13]. Cold spraying processes offers several advantages

* e-mail: soyinbo@uj.ac.za

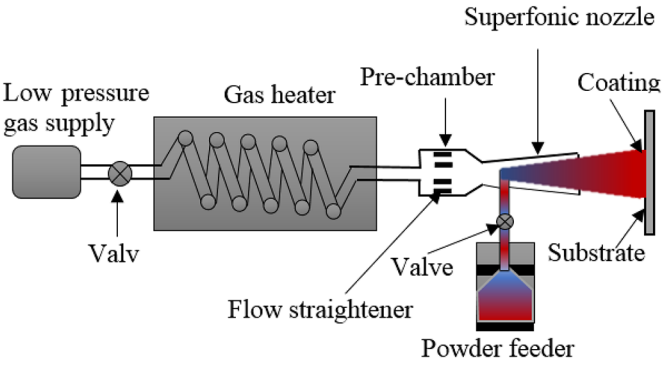

Fig. 1. Fundamental concept of low-pressure pressure cold spraying (LPCS) [19].

both in the processing itself and in the deposition result. Such advantages are: ability to protect materials against corrosion, increase wear resistance and mechanical durability, create components with different thermal and electrical conductivities than substrate would yield, or producing coatings on the substrate components as thermal insulators, high fatigue strength coating, prohibiting creep in an environment with high temperature, clearance control, restoration and repair, prostheses with improved wear, and produce components with attractive appearance [14–17]. These make cold spraying processes industrially commercialized because of its wide range of applications in aerospace- repair of solid rocket boosters space shuttle, aircraft industry, gas turbine, petrochemicals, electronics, bioengineering, casting, oil and gas, automotive industry, etc. [17].

Several deposition parameters have been investigated to obtain a wide range of deposits of powder particles. Therefore, it is necessary to gather a comprehensive database with the overall processing conditions. This study focuses on the review of those existing numerical and experimental deposition processes. It includes in the next section the concept of cold spraying (Sect. 2), and then Section 3 addresses the technology involved in the CGDS system, coating formation and deposit development. Afterwards, Section 4 addresses thoroughly the various process parameters of CGDS. Recent CGDS applications are also reported in Section 5. Conclusion and prospective future advancement are outlined in Section 6.

2 Conceptualization of cold spraying

Presently, cold spraying is categorized into two types based on the method of powder injection into the nozzle throat namely low-pressure cold spraying (LPCS) and high-pressure cold spraying (HPCS). Low-pressure cold spraying injected powder particles by the help of accelerated propellant gas at low pressure. LPCS system uses relatively low pressure ranging from 5 to 10 bars and pre-heated temperature of up to 50 °C of nitrogen, helium or free available air as a propellant gas, then forced through a nozzle. The pre-heated gas accelerates at a speed between 300 m/s and 60 m/s. Figure 1 shows the LPCS system in which the solid powder particles radially introduced from the system powder feeder downward and accelerated through the nozzle toward the base material (substrate) by venture effect [13,19,26,]. The pressure is kept constant below the atmospheric pressure within the nozzle. This can only be achieved if the equation $A_i/A_t \geq 1.3P_0 + 0.8$ [18] is satisfied, where A_i (m^2) is the c nozzle cross-sectional area at the entrance, A_t (m^2), nozzle throat cross-sectional area and P_0 (MPa) is the nozzle inlet gas pressure. LPCS is more flexible, portable and experience a significant reduction in spraying cost than HPCS system which uses a high-pressure delivery system. on the contrary, LPCS method can only attain deposition efficiency below 50%. The Service life of the LPCS nozzle is longer because powder particles only pass through the supersonic area of the nozzle thereby reducing the wear of the wall of the nozzle. The high-pressure cold spraying (HPCS) forced powder particles with either air, nitrogen (N_2) or helium (He) as propellant gas through a De-Lavar nozzle at high pressure 25 to 30 bar and pre-heating temperature as high as 1000 °C. The heated gas accelerates to a supersonic region of about 1200 m/s at the same time reducing its temperature. As shown in Figure 2, at the pre-chamber zone, the propellant gas mixes with the powder particles and forces into the gas stream axially. The powder particles accelerate at 600 to 1200 m/s strikes the surface of the substrate with enough energy (kinetic) to induce metallurgical and/or mechanical adhesion. The HPCS system efficiency is more than that of LPCS and is up to 90% [18].

LPCS system and HPCS system discussed above have some limitations. LPCS with simpler equipment has relatively low exit Mach number (usually >3) due to the restriction in the design of the nozzle. Through downstream feeding techniques, only low particle velocities can be achieved because 1 MPa inlet pressure is allowed. The high-pressure particle feeders are large in size and very expensive. Nozzle clogging is another limitation especially when there is an increase in the velocity and particle temperature. This problem can be overcome by mixing a high yield strength particle or particle with a larger average diameter with the first powder particles. Another HPCS limitation is the particle erosion that occurs at the bonding interface which causes wear of the nozzle supersonic nozzle throat. This can be more severe when hard powders as feedstock are being sprayed. The basic cold spraying components are particle powders ranging from 1 to 50 μm in diameter, compressed gas source, gas heater, De Laval nozzle, spraying chamber and control system [18].

Recent research works were carried out on the development of Cold spraying (CS) process which includes the processes, technology and the principles it involves as well as the potential applications [20–22]. CS technology has some variations which have been introduced to aid its capabilities. Kinetic metallization (KM), a solid-state process is the first method introduced. This method uses a converging nozzle under a choked flow condition to achieve an exit gas velocity of Mach 1 by making the nozzle slightly divergent to minimize friction [22]. Other cold spraying methods used a De Laval nozzle to attain a supersonic speed of the propellant gas. Pulsed gas dynamic spraying (PGDS) is the second variation set up to CS [23]. The powder particles in this process are heated to a

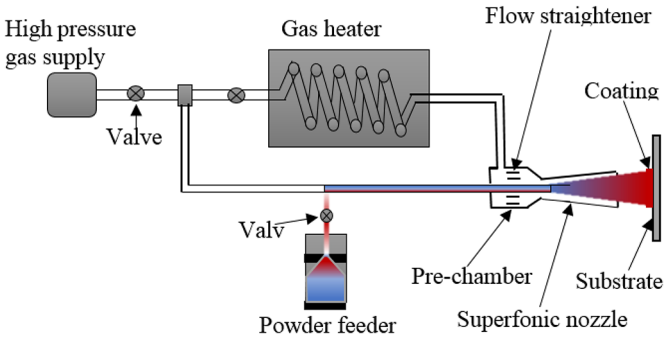

Fig. 2. Fundamental concept of High-pressure cold spraying (HPCS) [19].

temperature higher than the temperature experienced by the CS process but below the melting temperature. This method has high technological value by increasing the temperature to decrease the critical velocity. Impact velocity can also be maintained to yield a higher level of plastic deformation. This process makes use of moving pressure wave as a discontinuous nature to generate higher temperature and pressure at the same time than in CS process which makes use of continuous, stationary flow [24,25]. Vacuum cold spraying (VCS) is another CS variant. VCS operates at a pressure lower than the atmospheric pressure. At low pressure, the particles are fed into a vacuum tank. The vacuum tank provides an environment with low pressure in conjunction with the vacuum pump. Gas recovery and collection of waste powder particles are possible in the vacuum tank [1,25]. Aerosol deposition method (ADM) [27–29] is another variation technique similar to VCS. Nanoparticles are propelled by helium or air as a flowing gas in a vacuum chamber. The propellant gas in this process is at a pressure lower than atmospheric pressure and low velocity while comparing to CS. Deposition of small particle powder is possible because the shock wave or substrate bow shock effect is significantly reduced in this process. Different techniques of CS process is shown in Figure 3.

3 The technology of cold gas dynamic spraying (CGDS) process

3.1 Mechanism of CGDS system

Cold gas dynamic spraying (CGDS) can be used to produce both the bulk coating and thin-film coating. The coating is produced by a solid-state molecular attraction of particle/substrate impact at several hundred m/s high impact velocity. The basic components of CGDS systems shown in Figure 3, are the gas supply at high pressure, control module with gas heater, main gas (the propellant gas) from a gas control, the secondary gas (the particle feed gas) connected to a powder feedstock, substrate support system and the spraying component (workstation). Using different gases are possible by this configuration. The main gas supply source is connected to the De Laval nozzle at the pre-chamber gas spraying interface. Temperature and pressure are the propellant gas major input parameters which are the basic limit control of the system. These input parameters are regulated at the gas heater and the module regulator in the control system. The movement of the substrate support and the spraying component build and shape the powder deposition. This movement of the spraying component is controlled by a robot arm. The motion of the substrate support component can be restricted for curved or flat surface deposition. The component can also be allowed to move for the deposition on revolve surfaces. The revolve surfaces can either be asymmetric surfaces where the spraying component motion can be combined with the robot movement to produce 3D complex shapes or axisymmetric surfaces.

3.2 Mechanism of coating formation process

The formation process of the deposit is divided into two phases; the first layer formation which is the adhesion of the deposit onto the substrate and the build-up of the coating i.e. the growth of the deposit itself.

In the literature, several coating mechanisms that have been identified will be addressed in this section. The atomic bonding concept as evident in cold spraying and high impact welding is often used as a tool to explain bonding at solid-state but its behaviours during the high stain impact are yet to be known. Metallurgical bonding is most appropriate to describe the bonding nature since the impact enables transformation or structural changes at the region of the interface where there is emergent of a new interface and bonded zone features are characterized. Therefore, there is a relationship between the interface metallurgical response and the formation at the joint. In the CGDS literature, the fine characterization of the deposit/substrate interface has generally led to this statement and various metallurgical bonding phenomena have been suggested, including dynamic recrystallization and intermetallic formation, particularly for combinations of metals particle/metallic substrate [29].

A bonded zone recrystallization was showed in [31–33]. At the high strain rate impact, features of primary grain disappeared during the interface evolution. According to Zou et al. [32] analysis, a recrystallized joint formed at the interfacial zone produced nano-sized (new ultrafine grains) at the interface zone. The phenomenon described as "dynamic recrystallization" was used to describe the twining of the grain while strong hardening occurred at the interface due to high plastic deformation. The credibility of producing bond through this recrystallization phenomenon is unclear. Although at the interface, there was a distinct zone occurrence. The study carried out on combining titanium and aluminium as particle and substrate respectively by Rajafa et al. [33] revealed another recrystallization phenomenon. The evolution of heat confined during the impact of the deformation zone gave rise to this thermal phenomenon that was activated. Also, the conformity of structure lattice condition at the interface of titanium/corundum may be a prevalence of a hetero-epitaxy which are favourable to an impact enhancement. Experimental findings are in agreement with this verdict [33].

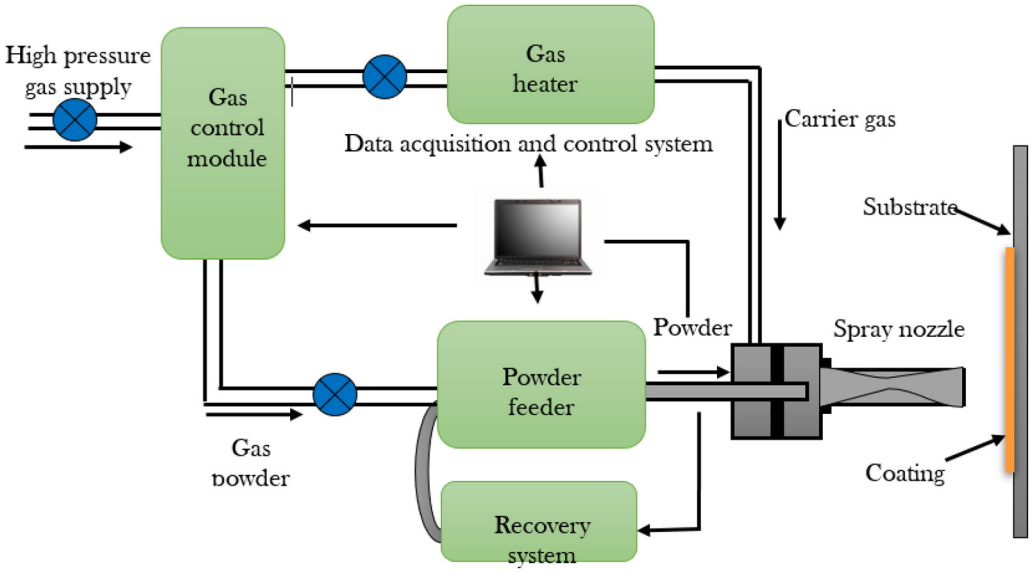

Fig. 3. Schematic of cold gas dynamic spraying set-up [30].

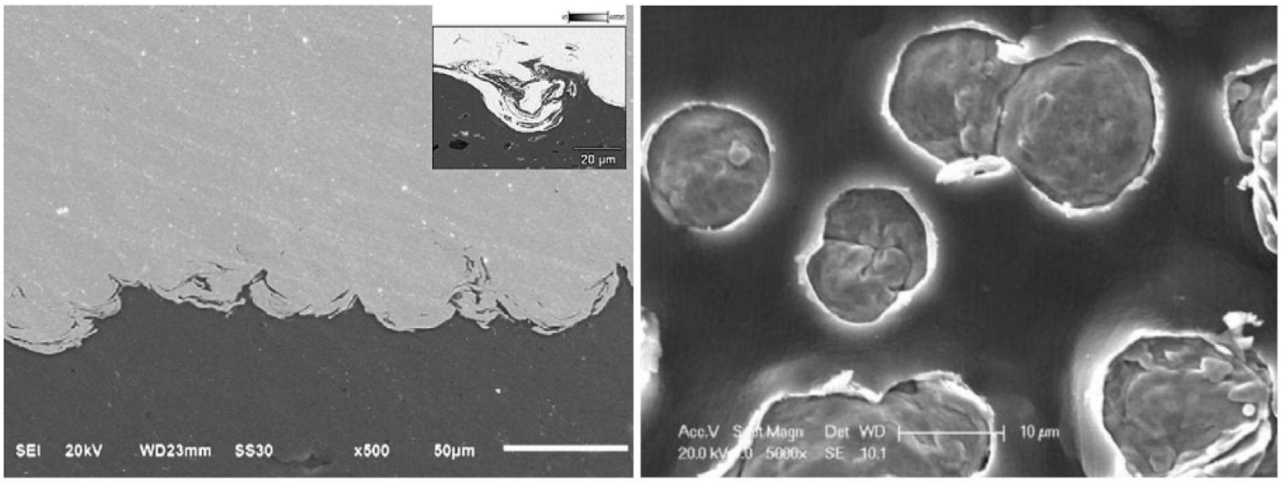

Fig. 4. Intermixing of complex material at Cu powder particles and Al substrate interface during (a) Cold spraying of Cu/Al surface [37], and (b) embedment of Cu/Al surface [32].

The strain localization at the interface plays a major role in the metallurgical nature of the bonded zone. Within the share region, interfacial sharing which is newly developed produces an adiabatic condition by high strain rate plasticity. This share region may be melted under severe plastic deformation thereby forming at solidification stage an intermediate layer. The intermediate phase changes the joint nature into a metallurgical bond via the intermetallic layer. The heat diffusion from the thermally confined zone towards the thermally non-affected large media decides the structural features of the intermetallic. The solidification can unexpectedly happen when the dissipation of heat at the confined heat zone passes through a cold conductive media. Contrary to the slow solid-state formation that yields rearrangement and migration of atoms during equilibrium transformation, this solidification that abruptly occurred produces an amorphous-like structure at the melted layer confined zone since at the initial position the atoms are frozen disorderly. Across the interface, the adiabatic shear band is observed to correspond to an amorphous structure/layer produced [35–37]. The collision that involved high strain problem like this metallurgical bonding case can be solved numerically.

During the collision, the interfacial deformation was responsible for the bonding of the particle and the substrate. The degree of deformation can be used as a tool to classify the bonding mechanism into three natures. In general, the mechanical bonding can be an interfacial mixing [38–40], an embedment in the substrate [12,41–43], or anchoring of particles on the substrate surface [34,44,45]. Complex deformation makes the interfacial mixing possible. Within the Interfacial affected zone, the intermixing of the powder particles and the substrate occur at the vertices as shown in Figure 4a. The generation of bulk deposit/

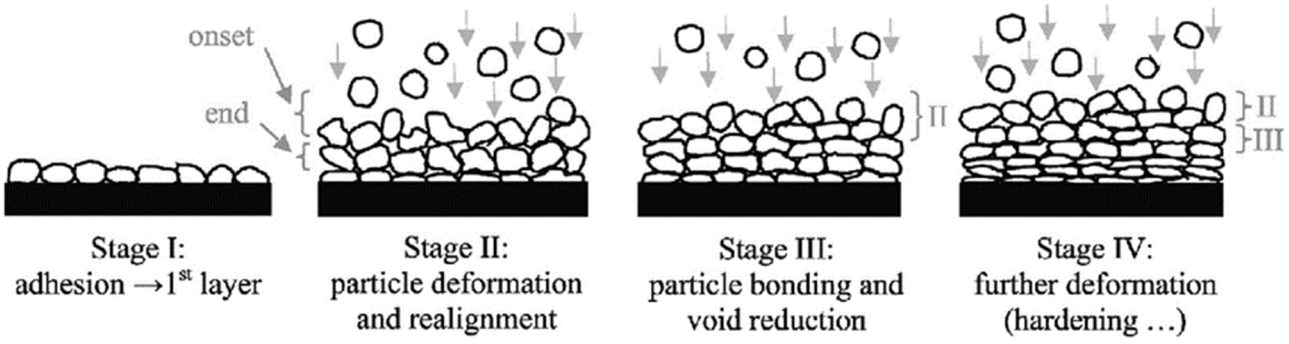

Fig. 5. Schematic diagram illustrating metallic particles deposit formation during CGDS [59].

substrate intermixed by swirling kinematic is due to this kind of specific morphology. Deposition of Cu/Al as particle/substrate is evidence of interface material mixing techniques and limited researches have been carried out on this subject as revealed in the CGDS literature. To produce interfacial mixing, substrate condition specification was presented by Champagne et al. [38] before the particle deposition can occur. The interfacial complex kinematics was not accounted for directly using this approach. However, the distinction from the contribution of an interlocking by embedment becomes tricky since a penetration of the particle in the substrate would create such a mechanical bonding. This mechanism of adhesion (mechanical embedment) has played a vital role in combinations of several materials as particle/substrate such as metallic/metallic [42], ceramic/metallic [41], oxide/polymer [45], as well as metallic/polymer [41,46,47]. An open surface that produces a metallic bonding through metallic powders partial embedment in the case of a non-similar combination of materials generates Metallic coating formation Figure 4b.

Weak penetration at the bonding interface is enough to generate an interlocking between the substrate and the particle without significant penetration. Metallic/glass combination is a typical example of this phenomenon [34,44]. It has been discovered that metal powders can impact and adhere to the roughened or smooth surface of a glass substrate. This had made angular particles such as copper powders to be mechanically onto a smooth glass surface or silicon rough substrate surface [43]. Some investigations on this bonding phenomenon covered in the literature described the adhesion of metallic powders and non-metallic particles (ceramics) [34,44,48,49]. It is worth noting that the apparent adhesion at the interfacial bonding zone of particle/ substrate experiences a variation of mechanical anchoring. At the bonding interface, it can be depicted that continuity in the material structure is observed suggesting a mechanical anchoring of the deposit within the imperfect surface structure of the substrate [12,39]. This deposit/substrate mechanical accommodation was perfect for combining polymer particle and metallic substrate [50,51], metallic/ceramic [48], and metallic/polymer [12,38,47,52]. In the case of polymer/metal combination, complete adhesion can be achieved when the deposition is heat treated. The build-up coating on the metal substrate was facilitated by the layer of the melted polymer [51].

3.3 Mechanism of coating deposit development

Coating deposit development is the second phase after the first layer adhesion, and this depends on the capacity of the deposits to be formed on the substrate. The behaviour of the mechanical structure of a particle/substrate during the impact determines the deposit cohesiveness. Presently, two consolidated natures have been predicted and this depends on whether or not the powders deformed plastically on the substrate [52]. The metallic bonding is achieved through ductile deformation while at the interfacial zone during deposition, the plastic deformation yields high impact. As stated earlier, the transformation of material structure activation is due to the serious plastic deformation while metallurgical bonding can be used to produce inter-particle cohesion. Van Steenkiste et al. [8] used this metallurgical bonding phenomenon to characterize ductile metals in coating deposit development. To enhance deposit consolidation after the formation of the first layer, the following stages were identified. The growth of the deposit starts by both particles rotational motion and deformation. This combination of the kinematics improves the density of the deposit. The second stage is where the inter-particle bonding occurs when the deposit plastically deformed onto the substrate. In this case, there is a decrease in the porosity. The last stage as observed by Van Steenkiste et al. [8], during characterization was the deposit densification that continues to increase the particle hardness. These mechanisms as shown in Figure 5 give a detail explanation of how ductile particles can be manufactured during cold gas dynamic spraying.

An alternative mechanism for coating build-up of non-ductile metals has been proposed [53]. Particles compactness governs the growth of ceramic deposit onto the substrate according to the investigation that was performed. The fragmentation of brittle particles occurs as the particles collide the substrate surface. Self-compaction deposits are achieved as the broken fragments pile up together by the impact. The deposit cohesion is observed. The deposit cohesion and densification are reinforced layer by layer by additive manufacturing. The deposit cohesion can also be enhanced by the angular geometry and fine small-sized features of the fragments [44]. By chemical bonding, interlocking at the interface may occur. This mechanism of stacking interlocking of non-metallic materials yielded final packed deposit. Nano-meter

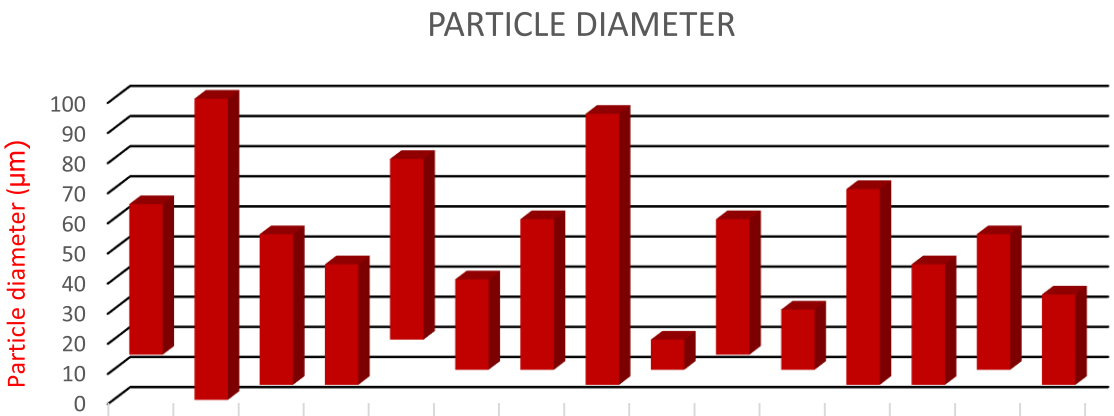

	Ag	Al	Cu	Ni	SS	Ta	Ti	Zn	Sn	Fe	Al-Sn	Al-Si	MCrAlY	WC-Co	Sic
MAX	50	100	50	40	60	30	50	90	10	45	20	65	40	45	30
MIN	15	0	5	5	20	10	10	5	10	15	10	5	5	10	5

Fig. 6. The typical range of powder diameters used for various materials in CGDS experiments [68].

coatings of thin Al_2O_3 [54], Y_2O_3 [44] and WO_3 [45,55,56] were produced, as well as up to 100 µm coatings of TiO_2 [54,57–59,62].

4 Process parameters of cold gas dynamic spraying (CGDS) process

There are several process parameters involved in cold spay technology since the deposit is determined by particles' size, morphology, and property, particle velocity and critical velocity, characteristics of the propellant gas, substrate surface roughening, preheating and texturing and as well as nozzle design. It becomes a difficult task for the experimental selection of major working /processing parameter as these parameters depend on one another. CGDS process is generally distinguished by the traditional thermal spray due to the practice of low temperature and pressure. This review provides a comprehensive and reliable baseline for the choice of process parameters used during CGDS.

4.1 Powder particles' size, morphologies and property

Powder particle's size is a major factor that contributed to the successful cold spraying deposition as well as the choice of typical particle size in practice. Generally, it is easier to accelerate and deposit a particle with sizes ranging from 100 µm and below while particles above this range always have difficulty to accelerate. It is therefore very paramount to be careful in the choice of particles' sizes. In general, the velocity of the particles (Vp) and the deposition efficiency (DE) can be reduced and optimized in order to obtain an optimum particle's size range. In the literature, the maximum particle size varies between 20 and 60 µm for several materials, except that aluminium (known as a light metal) and zinc (known as a soft metal) have been used with up to 100 µm and 90 µm, respectively as shown in Figure 6. The granule structure of particles is a factor upon which the deposition efficiency optimization depends. The distribution of powder particle size indicated by $f(dp)$ as suggested by Assadi et al. can be used to express the deposition efficiency (DE) as [60]:

$$\mathrm{DE} = \int_0^\infty f(d_p)dd_p. \tag{1}$$

Particle size optimization information can be used as a tool for obtaining the structure of the perfect granules of particles. Several formulae have been developed in the literature that can be used to predict the upper limit of the particles' size, but the challenge is, it cannot be used for the lower limit of particles' size. This is because smaller particles' size diameter responds sharply to the heat generated at the throat zone of the nozzle, bow shock effect and the thermo-mechanical adhesion of the particles on the internal wall of the nozzle. Chun et al. proposed a special design for the nozzle to curb the aforementioned limitations. The nozzle they developed was used for the deposition of copper particles of 5 µm size at normal propellant gas operating condition of pressure and temperature [61]. The result of their experiment revealed an appreciable increase in the deposition efficiency, increase in bond strength of the deposit and thickness of the coating. When using a conventional nozzle and fine powder particles, the poor deposition was achieved [61]. Furthermore, the interaction between the gas flow and the fine particles can cause particle self-agglomeration. Thereby, complex evaluation of deposit formation limiting behaviour is necessary for determining the minimum value of particle size. Several collections of particles' sizes from experimental work find in the literature are provided in Figure 6. The deposition of finely powder particles (submicronized) has also been investigated in the literature [59,63–68]. Particles' size ranging from 20 µm to 1.0 µm in the investigation makes use of very low temperature and low pressure for the deposit to be successfully deposited. These submicron particles flow through the nozzle by the acceleration of non-heated propellant gas in the process called vacuum deposition. Coating of materials with high

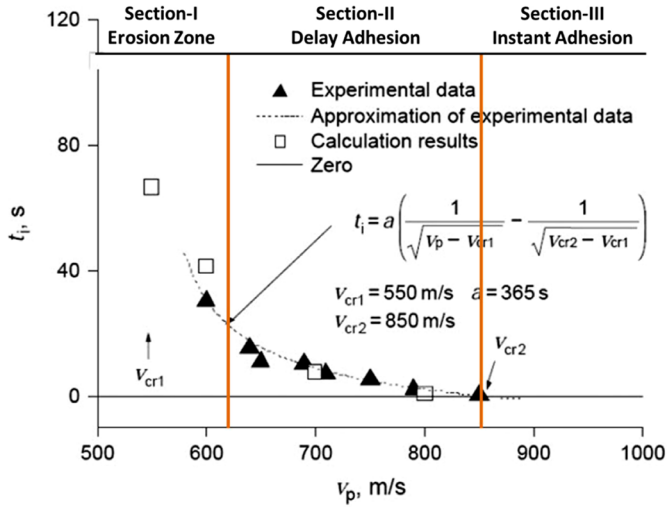

Fig. 7. Schematic diagram illustrating time vs. the mean impact velocity of Al particles on a polished Cu substrate [17].

thermal conductivity and structural component with fine porosity can be manufactured through this cold spraying variant.

4.2 Particle velocity and critical velocity

One of the important cold spraying parameters that generally influenced the deposition capability is the particle velocity (V_p) before impact. V_p also determines the state of plastic deformation at the particle/substrate bonding interface as well as substrate surface erosion. Critical velocity (V_c) is the minimum particle velocity for a given material that is enough to accomplish particle/substrate adhesion. Coating of deposited particles can only be achieved provided that the particle velocity exceeded the critical velocity [17,37–40]. Many researchers have proven that V_c changes with different powder particles. Materials such as Al, Ni, Fe, and Cu have respectively critical velocity of 680–700, 620–640, 620–6400 and 560–580 m/s [17,37–40]. This variation is however noticed when Cu particles were used as deposit materials at a critical velocity of 500 m/s Champagne et al. [38] and V_c ranging from 298 to 356 m/s was reported by Li et al. [73]. Figure 7 shows the induction time versus the mean impact velocity of Al particles on a polished Cu substrate with three distinct zones (i.e., zone-I, zone-II, and zone −III) in the account of two different particle velocities, V_{cr1} and V_{cr2}.

It can be deduced that many factors are responsible for this variation. Such factors are summarized in Table 1.

– particle/substrate thermo-mechanical properties;
– particle/substrate thermal properties;
– particle/substrate oxidation state.

Particle velocity V_p also is influenced by spraying conditions such as property and nature of propellant gas, particles' initial pressure and temperature, the geometry shape of the nozzle and several other properties (the diameter, size, morphology density etc.) of the material used.

4.3 Characteristic of propellant gas: type, temperature and pressure

Either air, nitrogen or helium is used as a major propellant gas in the cold gas dynamic spraying process. Helium (He) possesses a specific characteristic which makes it more efficient than Air and Nitrogen (N_2). Low molecular weight and higher gas constant (R_s) property of Helium makes it more preferable as shown in Table 2. The following expressions can be used to compute the Mach number (M) as a dependant of nozzle cross-sectional area, A/A^*, temperature ratio, T/T_0 and gas velocity, V

$$\frac{A}{A^*} = \frac{1}{M}\frac{2}{\gamma+1}\left(1+\frac{\gamma-1}{2}M^2\right)^{\frac{\gamma+1}{2(\gamma-1)}} \tag{2}$$

$$\frac{T}{T_0} = \left(1+\frac{\gamma-1}{2}M^2\right)^{-1} \tag{3}$$

$$V = M\sqrt{\gamma R_S T} = \frac{M\gamma}{\left(1+\frac{\gamma-1}{2}M^2\right)^{1/2}}(R_s T_0)^{1/2} = f(\gamma)(R_s T_0)^{1/2} \tag{4}$$

$$\frac{\rho}{\rho_0} = \left(1+\frac{\gamma-1}{2}M^2\right)^{\frac{-1}{\gamma-1}} \tag{5}$$

Specific gas constant (R_s) and specific heat ratio (γ) are related by equation (5). From equations (4)–(6), γ is influenced partially by Mach number (M) and $f(\gamma)$ for its value ranging from 1.4 to 1.66, an obvious velocity change can be found in $R_s T_0$ or R_s in the case of the three gases. The prediction of gas velocity based on the expansion ratio of the nozzle and $R_s T_0$ was revealed using non-heated propellant gas. R_s ranges from 200 J/kg K to 2000 J/kg K and the value of T_0 is 293 K.

High velocity is produced when He is used to propelling the gas with better efficiency when compared to N_2 and Air whose velocity is low resulting from a low value of R_s. As stated earlier, particle velocity depends on a factor of propellant gas density and its velocity. The propellant gas density has a very weak effect of γ between 1.4 and 1.66. It can be deduced that one important parameter that determines the propellant gas and particle's velocity efficiency is the specific gas constant R_s. This means that with the use of Helium gas, critical velocity can be attained by the particles.

For metal required to attain very high critical velocities and for expensive materials, Helium is recommended [74]. Furthermore, Helium is not economically viable, and not freely gotten in comparison to Nitrogen and Air, although it has several merits such as deposit densification improvement, high productivity and working temperature increase [97–99]. Nitrogen and Air used more in managing the cost of manufacturing. Air oxidizes, unlike Nitrogen which prevents sample oxidation.

Table 1. CGDS coating build-up stages and its V_p and V_c relationship.

Initial stage /first stage	Second stage	Third stage
Delay time or induction time. This is the time interval at the start of surface treatment when the particle flows and at the commencement of particle/ substrate adhesion [17].	First thin layer coating occurs at this stage. Plastic deformation and adhesion of particles onto the substrate occur	Surface interaction occurs at this stage. The deposition formed in the previous stage interact with the current particles. This stage is characterized by the build-up coating layers [17],
If $V_p < V_c$, the particles jump off the substrate surface [69]. If $V_p = V_c$, erosion occurs at the substrate surface without any evidence of deposition	V_c depends on the particle/ substrate combinations [70].	V_c at this stage involves the combination of particle/ substrate impact where both the powder materials and the substrate are of the same composition.
As shown in Figure 7, three velocity regions are evident: V_{cr1}, V_{cr2} and V_p [17]. If $V_p < V_{cr1}$, multiple particles impact the substrate before adhesion can occur.	If $V_{cr1} < V_p < V_{cr2}$, then adhesion occurs after some time. $V_p > V_{cr2}$ (850 m/s), particles adhesion rapidly occurs.	Higher erosion occurs due to up-limit velocity at this stage. If up-limit velocity is greater than V_p, build-up coating is achieved. The up-limit velocity of most powder particles is greater than 1000 m/s [70].

Table 2. Air, nitrogen and helium specific gas constant (R_s) and the specific heat ratio (γ).

	Helium (He)	Nitrogen (N_2)	Air
Specific heat ratio, γ	1.66	1.4	1.4
Specific gas constant, R_s(J kg^{-1} K^{-1})	2077	297	287

Materials requiring pressure up to 5 MPa have their pressure antemperature of their propellant gas. Gases usually need to be pre-heated between 20 °C and 800 °C temperature. In Table 3 are the details of materials pre-heated temperatures. For example, the deposition of cermet compound (e.g. Nickel-based alloy and MCrAlY compound) required a very high temperature ranging from 500 °C to 800 °C. Low pressure and temperature conditions are required for oxides and ceramic to be deposited, basically greater than 2 MPa and 300 °C. Deposition pressure of about 4 MPa is required for Nickel. Soft metals such as Zn and Sn require low pressure and temperature, while relatively hard metallic materials such as Al, Cu and Ti can be deposited at the same working conditions using Helium as propellant gas, only that higher pressure and temperature are needed for air or nitrogen gas. High pressure and temperature are required for titanium-based alloy and stainless steel for successful adhesion. The propellant gas' inlet pressure and the temperature influences the particle's kinematics during the cold spraying processes. Particles in the nozzles are to be injected by the propellant gas, that's its main function, and as such injection, pressure and temperature are required to below as the propellant gas inlet temperature and pressure. There would be a resulting increase in the temperature and pressure within the convergent zone of the nozzle if there is an increase in the pressure and/or temperature of the propellant gas, subsequently, particles attain a high velocity and temperature resulting in the efficiency in deposition and adhesion deposit strength [77]. Further increase in pressure of propellant gas can have a negative effect on the gas flow kinematics especially at a higher temperature of the propellant gas. At the nozzle throat upstream, there would be a significant decrease in gas temperature when combining the gases with such temperature difference thereby resulting in temperature drop by limiting the gas kinematic capability. The deposition of particles is now less efficient and lesser when the mixing of temperature is promoted by the carrier gas injection pressure [78].

4.4 Substrate surface roughness effects on particle/ substrate adhesion

The adhesion of cold spraying particles is greatly dependant by the condition of the substrate surface, considering the temperature and its topology. Presently, three major areas have been identified in the publications to categorize this subject into the effect of substrate thermo-property, surface roughness and surface texture. Good bonding is believed to be attained with a well-prepared surface, free of oxidation and contaminants during cold spraying. Invariably, earlier deposition and preparation of substrate surface are advised. For glass and

Table 3. Details of process parameters.

Particle	Substrate	Propellant gas	Particle diameter (μm)	Temperature (°C)	Pressure (MPa)	Nozzle throat diameter (mm)	Nozzle length (mm)	Ref.
Ag	$SS347_{(grit\ blasted)}$	Air	15–50	250–450	1–2	–	–	[92]
Al	$Al_{(pickled)}$	He	20	20	1.5–2	–	–	[93]
Al	Al	–	2–20	–	–	–	–	[94]
Al	$Al2024\ T351_{(grit\ blasted)}$	N_2	5–50	230	3.45	2	168	[95]
Al1100	Al1100	He + N_2	1–30	227–527	2.1	–	–	[96]
Al2618	$Al_{(grit\ blasted)}$	He	<25	20	1.7	–	–	[97]
Al2618	$Al6061_{(grit\ blasted)}$	He	25–38	20	1.4	–	–	[98]
Al7075	$Al5052_{(grit\ blasted)}$	N_2	–	500	1.6	2	–	[99]
Al	AZ91 Mg	He	15	200	0.62	–	–	[100]
Al	$AZ91D_{(sand\ blasted)}$	Air	1–40	230	1.6	2 × 4	–	[101]
Al101	$AZ91D_{(grit\ blasted)}$	He	6–174	300	0.98	–	–	[102]
Al	$Brass_{(sand\ blasted)}$	Air	40; 60; 80	204–371	2	3	80	[103]
Al	Ni	Air	∼80	280	0.7–2.5	1	–	[104]
Al	Sn	He	15–75	20	2.5	–	–	[47]
Al	Cu	✓	✓	✓	✓	–	–	[47]
Al	Al6063	✓	✓	✓	✓	–	–	[47]
Al	Brass	✓	✓	✓	✓	–	–	[47]
Al	Bs B01	✓	✓	✓	✓	–	–	[47]
Al	SS1040	✓	✓	✓	✓	–	–	[47]
Al	Al_2O_3	✓	✓	✓	✓	–	–	[47]
Cu	$Al6061_{(polished)}$	N_2	–	300	1.5	–	–	[82]
Cu	$Al6082_{(polished)}$	He	5–25	20	3	1.35		[105]
Cu	$Cu_{(grit\ blasted)}$	Air	75	500	2.5	–	–	[106]
Cu	$Cu_{(grit\ blasted)}$	He	1.32	–	–	–	–	[107]
Cu	Cast iron	N_2	1–50	600	2.7	–	–	[108]
Cu	$SS400_{(grit\ blasted,\ polished)}$	Air	5–50	300	3	2	50	[109]
Cu	$SS\ AlSI304_{(polished)}$	Air	5; 10; 15	250–650	0.4–1	2	130	[110]
Cu	$Al6063_{(polished)}$	Air	5; 10; 15	250–650	0.4–1	2	130	[110]
Cu	$SS\ AISI\ 304_{(4000C\text{-}Polished)}$	He	5; 15	20; 400	0.2–1	2	130	[110]
Inconel 625	$SS\ 304_{(grit\ blasted)}$	N_2	38–15	500	3.2–3.3	–	–	[111]
Inconel 718	$Mild\ steel_{(grit\ blasted)}$	N_2	33	800	3.5	–	–	[112]
Ni	$Steel_{(grit\ blasted)}$	N_2	5–22	600	3	–	–	[32]
SS 304	$Steel_{(Interstitial\ free)}$	N_2	52	450–550	3	–	–	[113]
SS 316L	Al	N_2	18–25	500	4	–	–	[114]
SS 316L	Al	N_2	28–45	600	4	–	–	[114]
SS 316L	Al	N_2	36–53	720	4	–	–	[114]
SS 316L	$Al7075\ T6_{(pickled)}$	N_2	20–40	600–800	2–4	–	–	[115]
Ta	$Al_{(cleaned)}$	N_2	10–30	800	3.8	–	–	[116]
Ta	$Steel_{(grit\ blasted)}$	N_2	10–30	800	3.8	–	–	[116]
Ti	$Al_{(grit\ blasted)}$	N_2	–	370–480	2.7	–	–	[117]
Ti	Al6063 TS	He	22	600	1.5	–	–	[118]
Ti	Al_2O_3	N_2	25	450	2.5	2.7	–	[33]
Ti	$Mild\ steel_{(sandblasted)}$	N_2	38–44	155–263	2	2	100	[71]
Ti	$Mild\ steel_{(polished)}$	He	38–44	255	1	2	100	[71]
Ti	$Iron_{(polished)}$	He	<25	20	2.9	1.35	100	[80]
Ti	$Mild\ steel_{(polished)}$	He	<25	20	2.9	1..35	100	[80]
Ti	$SS\ 304_{(polished)}$	He	<25	20	2.9	1.35	100	[80]
Ti	$Martenstitial\ free_{(sandblasted)}$	N_2	44	450	2	2	100	[119]

Table 3. (continued).

Particle	Substrate	Propellant gas	Particle diameter (μm)	Temperature (°C)	Pressure (MPa)	Nozzle throat diameter (mm)	Nozzle length (mm)	Ref.
Ti	Ti	N_2	29	300–800	3; 4	–	–	[119]
Ti	Ti	N_2	16; 22	600	2.4	–	–	[120]
Ti	Ti	He	16	600	1.5	–	–	[120]
Ti	Ti6Al4V	He	5–29	260	1.6	3.8	90	[121]
Zn	$Al6061_{(grit\ blasted)}$	He	17; 45	260	2	–	–	[122]
Zn	$Zn_{(polished)}$	N_2	5.2–26.4	320	2	2	100	[123]
Zn	$Mild\ steel_{(grit\ blasted)}$	He	5.2–26.4	140	0.5	2	100	[123]
Zn	$Mild\ steel_{(grit\ blasted)}$	N_2	5.2–26.4	165–410	2	2	100	[123]
Al2319	$Mild\ steel_{(sand\ blasted)}$	Air	<63.8	250	2.8	2.7	170	[124]
Ti	$Mild\ steel_{(sand\ blasted)}$	Air	<38.9	250	2.8	2.7	170	[124]
Cu	$Mild\ steel_{(sand\ blasted)}$	Air	<98.5	250	2.8	2.7	170	[124]
Al	$Steel_{(33\text{-}3300C\ grit\ blasted)}$	N_2	36	33–500	0.6	–	–	[125]
Zn	$Steel_{(33\text{-}2450C\ grit\ blasted)}$	N_2	13	33–500	0.6	–	–	[125]
Sn	$Steel_{(33\text{-}800C\ grit\ blasted)}$	N_2	10	33–80	0.6	–	–	[125]
Al	Al	Air	53–75	315	2	2.8	–	[126]
Zn	Al	Air	45–	315	2	2.8	–	[126]
Al	Al	Air	90	290–340	1.5–2	2.8	–	[127]
Al	Bronze	Air	9–40	290–340	1.5–2	2.8	–	[127]
Fe	Al	Air	≤45	480–590	1.5–2	2.8	–	[127]
Fe	Bronze	Air	≤445	480–590	1.5–2	2.8	–	[127]
Cu	Al	Air	≤445	480–590	1.5–2	2.8	–	[127]
Cu	Bronze	Air	≤445	480–590	1.5–2	2.8	–	[127]
Cu	Cu	N_2	10–33	150	1	2.6	–	[128]
Cu	316L SS	N_2	10–33	150	1	2.6	–	[128]
Ni	Cu	N_2	10–33	150	1	2.6	–	[128]
Cu	$SS_{(sand\ blasted)}$	N_2	15–37	220	2	2	100	[129]
Ti	$SS_{(polished)}$	N_2	37–44	240	2	2	100	[129]
SS 316L	$SS\ 304_{(grit\ blasted)}$	He	16–44	150–300	1.5–3	–	–	[130]
Iron 101	$SS\ 304_{(grit\ blasted)}$	N_2	15–44	200–300	1–3	–	–	[130]
Ti	$Mild\ steel_{(grit\ blasted)}$	air	5–45	250	2.8	2.7	170	[131]
Ti	$Mild\ steel_{(grit\ blasted)}$	N_2	5–45	263	2	2	100	[131]
Ti6Al4V	$Mild\ steel_{(grit\ blasted)}$	Air	5–90	520	2.8	2.7	170	[131]
Al	$Mild\ steel_{(grit\ blasted)}$	Air	5–63	520	2.8	2.7	170	[131]
$Al\text{-}12Si_{at\ 1500C}$	$Al6061\ T6_{(grit\ blasted)}$	He	5–65	500	3	–	–	[132]
Al-5Sn	$Steel_{(grit\ blasted)}$	He; N_2	20	300	0.7	–	–	[133]
Al-5Sn	Al6061	N_2	20	500	3	–	–	[133]
Al-10Sn	$Mild\ steel_{(grit\ blasted)}$	He; N_2	15	300	0.7	–	–	[133]
Al-10Sn	$Cu\ _{(pickled)}$ $Al6061(_{(pickled)}$	He; N_2	15.2	300	0.7	–	–	[134]
Al-20Sn	$SUS304\ _{(pickled)}$	He; N_2	13.8	300	0.7	–	–	[134]
Al-13Co-26Ce	$Al_{(grit\ blasted)}$	He	23	200–370	1.7	2	–	[135]
Cu-2Ag-0.5Zr	$AlSl\ 4130_{(grit\ blasted)}$	He	27	500	1.6–2.6	2.7	–	[136]
CuCrAl	GRCop-84	He	10–25	300–500	1.5–2.5	–	–	[137]
Cu-Sn	$SS_{(sandblasted)}$	He	48	520	2	2	100	[138]
Cu—6Sn	Mild steel	Air	28	500	3	6	170	[139]
Cu-8Sn	Mild steel	Air	17	500	3	6	170	[139]
Diamalloy	$Mild\ steel_{(polished)}$	N_2	<50	800		–	–	[140,141]
$T_{i2}AlC$	Al6061	N_2	25–40	500–800	3.8	–	–	[142]

Table 3. (continued).

Particle	Substrate	Propellant gas	Particle diameter (μm)	Temperature (°C)	Pressure (MPa)	Nozzle throat diameter (mm)	Nozzle length (mm)	Ref.
$T_{i2}AlC$	$Steel_{(grit\ blasted)}$	N_2	25–40	600–800	3.4–3.9	–	–	[142]
Al_2O_3	Al_2O_3	Air	0.5	20	0.4	1 × 1	5	[143]
SiC	$Inconel\ 625_{Cleaned}$	Air	6–33	280	0.6–0.8		–	[41]
WO_3	Si	He	30–50	300	0.7	4 × 6	–	[44]
PPA	HDPE	Air	150–250	20	0.075	5.2	200	[51]
CoNiCrAlY	$Al6061_{(grit\ blasted)}$	He	5–37	550	2	2	270	[144]
MCrAiY-Re	$Ni_{(cleaned)}$	N_2	10–40	800	4	–	–	[145]
WC-12Co	$SS_{(sand\ blasted)}$	N_2	9; 13; 17	750	2.4	2	100	[146]
WC-12Co	WC-12Co	N_2	9; 13; 17	750	2.4	2	100	[146]
WC-12Co	$Al7075\ T6_{(polished)}$	N_2	10–30	800	3	–	–	[146]
WC-17Co	$Al7075\ T6_{(polished)}$	N_2	10–30	800	4.4	–	–	[146]
WC-12Co	$SS\ SUS\ 304_{(grit\ blasted)}$	N_2	15–45	700	3.4	–	–	[147]
WC-17Co	$SS\ SUS\ 304_{(grit\ blasted)}$	He	15–45	600	1.2–1.5	–	–	[147]
WC-17Co	$SS_{(cleaned)}$	He	∼30	600	3–4	–	–	[148]
WC_25Co	$Al7075\ T6_{(polished)}$	N_2	32	800	3–4	–	–	[149]
WC_25Co	$Steel_{(polished)}$	N_2	32	800	3.4	–	–	[149]
WC_CoCr	$Al_{(grit\ blasted)}$	He	34 ± 17	550	1.7	–	–	[150]

polymeric substrate, cleaning and degreasing steps are mostly used. Grinding or polishing, grit blasting and sandblasting are the typical practices used for metals. To achieve an oxide-free surface, sand and grit blasting can be used also in attaining a roughened fresh surface also known as an activated surface. An activated surface ensuring that the particles can freely attach itself to the surface conveniently while non-activated surface aids particles rebound. The term was majorly used for the metallic substrate and its activation factor correlates with the roughness of the surface. Some positive effects of surface roughening were discovered in the literature on the bonding formation [6,73–75] while others say the exert opposite [75,76]. This leads to an analytical discussion on the effect of roughness on adhesion. Various combinations of particle/substrate have different surface preparations that are best for them. For example, Wayne et al. carried out a study on the impact of titanium particles onto a sapphire substrate to check for the effects of roughness on the adhesion [83]. The polished substrate that had a roughness of less than 3 nm was improved to having an adhesion coating thickness of 250m when compared to another substrate which produced a non-uniform coating of 150 μm. This tendency is also favourable for various other metals combination [6,73–75]. Although, polished and ground surface produced a comparatively bonding strength of the deposit as well as the mitigation of the strength by surface grit blasting (Fig. 8). The discontinuous contact at the bonding interface as recorded by Yin et al. resulted in about 24% decrease in bonding strength for grit-blasted surface [79]. It is observed that this imperfect bonding is seen only for particles with a size close to cavities sizes that grit blasting produced whereas larger powder particles are required as feedstock powders than that of the cavities. Hussain et al. in their investigation discovered a reduction of the bonding strength of 0.05 μm. for polished surface and 3.9 μm. for rough surface [80]. The oxides removal is being prevented during the impact and this is because interfacial jetting is hindered by the roughness according to their experimental observations. Hence, metallurgical bond formation is obstructed by disturbing the process of automatic surface cleaning [80]. Hence, the automatic surface cleaning during the process is disturbed and it eventually obstructs the formation of a metallurgical bond. Although the negative effect on the strength of the bond caused by the roughness is not a model as agreed by some studies (Fig. 9). Contrarily, there are suggestions from many authors that adhesion can benefit from this surface roughness [73–75]. Richer et al. in their investigation discovered that coarse grit blasting of Al-Mg particles impact with an improvement in the deposition efficiency on Mg substrate [82]. Substrate roughness favourable conditions have been identified by Wu et al. They discovered that at low deposition velocities, Al-Si particles show a flawless deposition when impacted a grit-blasted mild steel while under the spraying conditions it was difficult to achieve coating on a polished substrate [81]. In both cases, a comparison was drawn on the bonding strength for the onset deposit to be successful. The bonding strength decreases due to a range of roughness as a result of an increase in impact velocity which causes an incomplete compact between particle/substrate interface. When high impact velocity is attained enough to cause deformation of particles onto the substrate with roughened surface, roughness negative effect decreases, and it can disappear completely and thus improving mechanical interlocking to enhanced continuous bonding at the interface.

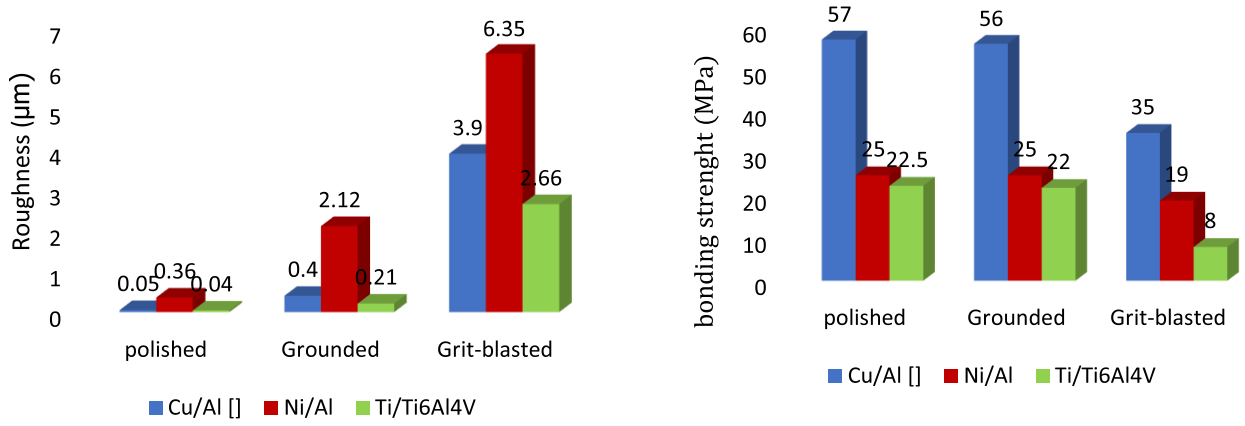

Fig. 8. Surface roughening and bonding strength effect in CS for Cu/Al [80], Ni/Al [79] and Ti/Ti6Al4V [6].

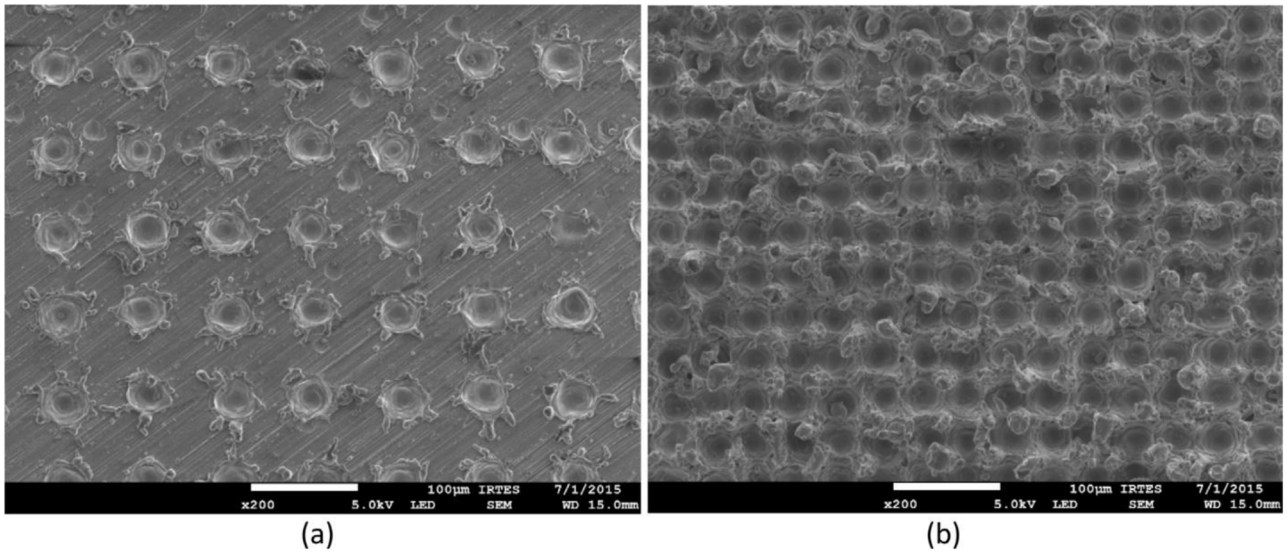

Fig. 9. Schematic diagram of weakly and highly surface texture of the Al surface pattern during the lesser texturing procedure: (a) Texture A and (b) Texture B [85,86].

4.5 Substrate pre-heating effects on the particle/substrate adhesion

The focus of some researchers is on the substrate pre-heating influence on the deposition. The deposition of soft, medium and hard particles as feedstocks was investigated by Legoux et al. using Sn, Zn, and Al. The pre-heating of carbon steel (grit blasted) was carried out at a temperature of 350 °C. During the deposition, the surface temperature was measured by Therma-CAM SC3000 (an infrared high-speed camera). It was discovered that the deposition efficiency (DE) decreases for Zn, increases for Al and remains constant for Sn. When performing a microstructural investigation on the sample deposit, Zn particles experienced an elongation and high impact adhesion. Although it suffered from oxidation while Al Particles experienced high impact deformation. Pre-heating effect for the Sn was not conclusive due to erosion at the substrate bonding zone with an unfavourable gas condition. Cu was deposited onto the pre-heated substrate of stainless steel and aluminium by Fukumoto et al. their result gives 0.3 µm. roughness in both cases. To avoid the propellant gas additional thermal effects, the gas was not preheated in their finding. They obtained an improved deposition efficiency in their experiment as a result of increased substrate temperature. Under the same processing conditions of 5 µm. particle mean size, the gas pressure of 5 bars, and temperature of 600 °C, they achieved a deposition efficiency of up to 80% while a deposition efficiency of lower than 20% at room temperature was observed [87]. Although substrate pre-heating yields a low crater formation number, there is no further clarification on the deposition improvement mechanism. Numerical simulation was carried out by Yin et al. to understudy the particle/substrate impact behaviours to suggest some improvement on the deposition of the pre-heated substrate [79]. The interlocking mechanism is introduced to further embed the particles into the substrate by thermos-mechanical softening phenomenal. For pre-heating temperature between 100 °C and 600 °C of Cu/Cu combination, it was revealed that there was no significant change in the contact area. The mechanical interlocking role is

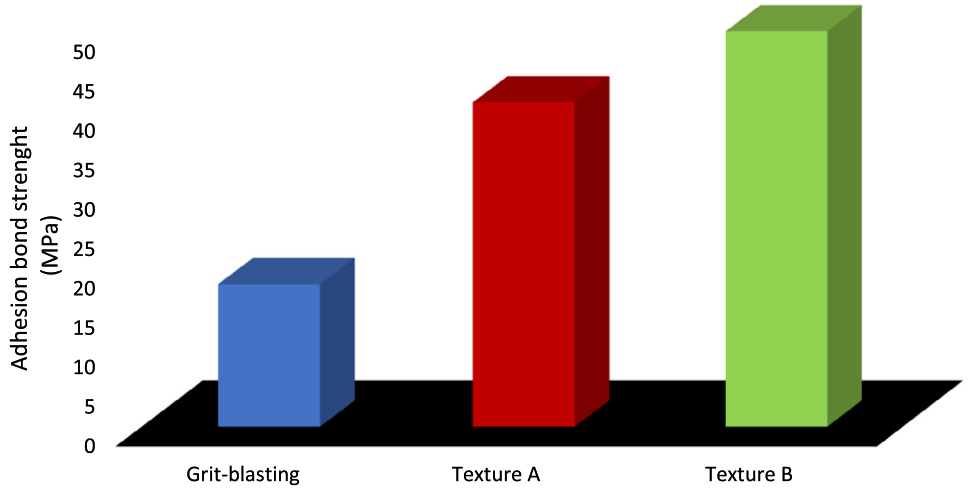

Fig. 10. Adhesion bond strength of Al/Al combination: Laser texturing effects [85,86].

limited in this situation as reported by the authors [88–91]. However, it can be inferred from the literature that substrate preheating plays a vital role in the thermos-mechanical softening during the cold spraying processes to promote adhesion [74–77]. Activation effect can be enabled by substrate preheating most especially when soft Cu particles are deposited onto a hard substrate such as Al_2O_3 [71]. The decomposition and evaporation at the interface of Al_2O_3 free surface occur when increasing the substrate preheating temperature leading to Cu/Al_2O_3 adhesion as metallic/ceramic deposition during cold spraying [84].

4.6 Substrate surface texturing effects on the particle/substrate adhesion

Surface texturing is a special novelty from the laser technology for surface preparation. Laser impulse high energy can produce on the substrate surface a high-fidelity pattern. To obtain various pattern on the surface, an automated canning method is used by the specific laser ablation procedure. The characteristic of texture surface generated by the laser treatment varies with hole orientation, the inter-hole distance and the hole depth and diameter by the laser impulse. An optimized shape and size pattern with a regular surface topography can be achieved by laser surface texturing. Kromer et al. use a laser texturing method to improve the adhesive behaviour of deposit [74]. Texture A and texture B are shown in Figure 10 for weak surface texture and a high surface texture respectively. The result generated from using the two textured surfaces during cold spraying is compared with 2.7 μm roughness of the grit-blasted surface. When those textured surfaces are used, the bonding strength increases by two or more (Fig. 10). The particle/substrate mechanical anchoring is improved by the texturing method. The holes of the pattern are filled by the deposit. Laser texturing method has proven an excellent bonding strength improvement of cold spraying coatings.

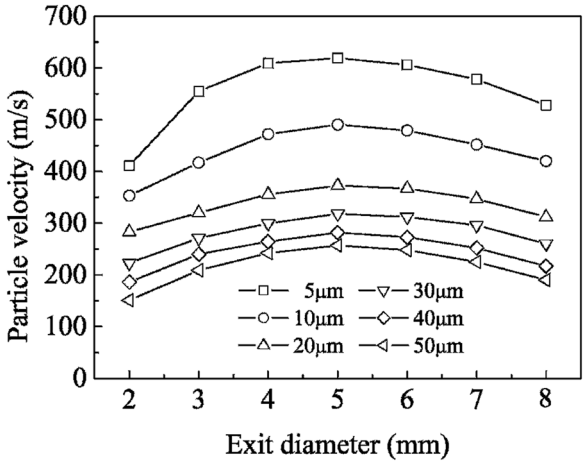

Fig. 11. Effect of nozzle exit diameter on the velocity of particles with different sizes using N_2 at a pressure of 2 MPa and a temperature of 300 °C [151].

4.7 Effects of nozzle unit design

The use of the dynamic model to improve the design of the nozzle has increased its capacity and performance. Hence, higher deposition efficiency and a denser coating are achieved. The nozzle design has a lot of influence on the particle velocity. The nozzle throat diameter, the exit diameter or expansion ratio inlet diameter influences the particle velocity. Nozzle's length has material and fabrication constraints that limit its application in practice. Therefore, new materials need to be tried to improve powder flow through the nozzle and optimization in design is required to minimize the gas flow through the nozzle [151]. Optimised nozzle design using tungsten carbide was used by Karthikeyan et al. [152] to coat GRCop-84 special alloy. The thermoplastic nozzle was designed by Champagne et al. [153,154,161] to deposit aluminium powder in order to correct the clogging effect of the steel nozzle. As shown in Figure 11, nitrogen gas was

used to accelerate particles at pressure and temperature of 2 MPa and 300 °C respectively with optimum 5mm nozzle exit diameter [151]. A special internal diameter spray gun was introduced by Li et al. and came up with 6.25 expansion ratio and 30 mm standoff distance for divergent nozzle 40 mm length. Helium and nitrogen gas was used as propellant gas. Their discovery shows that a deposit of dense coating can be achieved [72].

5 Applications of cold gas dynamic spraying (CGDS)

Cold gas dynamic spraying (CGDS) technology is a supplement to other known thermal sprays and so it is not a replacement either for any of them [155]. In the field of automotive, electronics, aerospace, medical and petrochemical industries, its applications help a great deal [13]. The CGDS applications remove any defects easily without extra cost on the production quality. For instance, the applications could help in repairing of cast or machine defects and so on saving the production. This process makes mould casting become easy.

CGDS is also widely used as a mechanics for restoration to promotes the renewal of antique objects both technical such as cars, aeroplanes, and art such as metal sculptures [156]. It is worth noting that in aerospace industries, Al and Al alloy coatings for space shuttle boosters are carried out by this spray technique for repair/refurbishment. It also acts as corrosion reducing agent in anti-skid coating [69], asides, it also offers corrosion protection coatings in petrochemical and in the gas turbine cast part. In-vehicle repair platforms [156] and automotive workshops, CGDS coating helps to eliminate associated defects, shape restoration and sealing of leakages [8]. It is also useful in coating solid surfaces and copper alloys such as bed rails, faucets, light switches, doorknobs, food preparation areas, and other hardware which are in contact with human frequently [157]. This coating technique also finds its application in the manufacturing of titanium pipes (seamless).

CGDS acts as an anti-seizure coating when treating welding lines, propeller shaft in the marine ship, and in oil-well tubing. It is also useful in the production of optical glasses elements [156]. With the help of this coating process, it is easy to service old equipment, expensive, scarce and worn out parts as well as removing defects without considering the cost of restoration in paper roll industries [156].

Vehicles air conditioning equipment and Al-tube heat exchanger can be fabricated by cold gas dynamic spraying. This process can also be used to produce high thermal insulators as well as high corrosion resistance components with less cost of manufacturing [158].

In the shipbuilding and automobile industry, sliding bearing materials make use of Al-Sn alloys. Sn provides a shear surface and suitable friction properties in the aluminium matrix due to its soft phase during sliding and its coarsening effects helps in the high-temperature environment. Al-10Sn and Al-5Sn coatings were successfully obtained by Ning et al. [133] through CGDS process with well-bonded structures and low porosity. Al-5Sn friction phase is consistent with cold spraying high-pressure process using nitrogen as propellant gas whereas, with helium as propellant gas, the deposition of Al-10Sn can only be achieved by low-pressure cold spraying [105].

CGDS can be used to improve component surface performance in power generation, especially in solar cells by fabricating complex conductive patterns. The Metallic or ceramic substrate can have aesthetic effects aids by this process [13].

Hydroxyapatite, HAP ($Ca_{10}(PO_4)_6(OH)_2$ in medicine can be used to coat several substrates [13]. The Crystallographic and chemical property of HAP similar to bone minerals makes it suitable for orthopaedic and dental implants. The absence of cytotoxic effects also makes HAP bonds directly to the bone. For surgical implants mechanically, strong metals are combined with bioactive HAP coating and this is due to its weak mechanical strength. Plasma sprayed technique is normally used for bio-ceramic coating but because of its high-temperature deleterious effects, cold spraying coating at low temperature can be used to eliminate these harmful effects. ASB industries successfully deposited Ti-HAP composite coating using 'CGT Kinetics 4000 cold spraying system'. The bonding strength is far better compared with plasma coating and hence, deposition of up to 30% HAP composition of dense composite coatings can be obtained by this technique. CGDS has grown for selected applications as viable alternative cold spraying methods to that of thermal spray [80,158,159].

CGDS technology can also coat GRCop-84 substrate successfully using NiCrAlY and CuCrAl particles with a tungsten carbide nozzle specially designed for this deposition. At NASA Glenn Research Center (GRC), Cu-8CR-4Nb and GRCop-84 were developed to produce fatigue and high-temperature creep capabilities in liner application of rocket engine. Bleaching is prevented by additional oxidation protection for their maximum life [160].

CGDS application extends its usefulness in the production of fixed-wing aircraft and helicopters transmission gearbox using aluminium barrier coatings to restore dimensional tolerances of heat-sensitive materials such as Mg alloys ZE41A-T5. MH-60S Seahawk and UH-60 Seahawk are a typical example. Structural metals like Mg are very influenced by galvanic corrosion due to its most active electrochemical nature when another metal is in contact with it. And also this alloy can be damaged when subjected to excess heat if thermal spray method is used to coat the alloys, then molten metal can react with Mg [93,94,160]

CGDS coating can be applied to power generation station. The coatings offer cavitation wear resistance in the case of wear rings, impeller seal section, impeller fins, water pump housing, turbine blade and protect the boiler tubes from high-temperature corrosion. Ni–Cr, chromium oxide and tungsten carbide CS coating are the preferred CS coating on these parts. Cold spraying at low temperature can be used to reconditioned wear rings by bronze coating. Coal crusher journal can also be coated with chromium carbide [162].

Electric mains aluminium tips can be coated with copper powder to protect transformer copper components by removing the electrochemical oxidation of the elements using this coating method. This technique can also be applied to automotive batteries with copper and aluminium wire terminals [162].

6 Conclusions and prospective future advancement

The cold dynamic spraying (CGDS) method, apart from evolving as one of the embracing powder deposition spraying processeses with a notable research finding including the basic evolutions introduced in Russia by the institute for theoretical and applied mechanics in 1980s, has significantly grown over the years and with the integration of De Laval nozzle as an innovative contrivance. Many researchers have characterized various phenomena involved during the coating formation process and coating deposit development.

The CGDS' enormous capabilities were revealed and identified through the collection of available data in the literature from the numerical, experimental and several distinct mechanisms. Based on the capability of CGDS to deposit and to use several materials combinations, the method is systematically classified to form a comparative review of the concepts and mechanisms of cold dynamic spraying systems, coating formations, building up developments, computational simulation approaches to CGDS, process parameters, including powder particle types, size and morphology, particle and critical velocity, propellant gas characteristics, substrate surface roughness and material properties.

CGDS experimental processing conditions such as approximately 800 °C and 5 MPa for temperature and pressure respectively have led to the deposition of metals of micron sizes powders. The mostly used propellant gases is the air, N_2 and He for the deposition. Due to low molecular weight and high specific gas constant, the most efficient one is He. At sub-atmospheric pressure without preheating the propellant gas in the vacuum chamber, the deposition of small size particles is possible. From 20 nm to 5 μm fine powder particles depositions are best done under those conditions.

Powders specific features in the literature concerning CGDS are carefully reviewed. Such features are the particles' size, morphology and properties. Powder particles' size is a major factor that contributed to the successful cold spraying deposition as well as the choice of typical particle size in practice. Particles pre-heating also play a significant role during deposition to facilitate the bonding by modifying the powders mechanical properties. It can be inferred that particles' pre-heating decreases the critical velocity thereby aids adhesion. A comparative study was also performed on the particles' morphology. Angular or dendritic particles' morphology increases the coating harness, decreases the deposit porosity, as well as deposition efficiency improvement. Conclusively, the high drag coefficient in porous powders enables it to attain the highest impact velocity and high deposition efficiency possible for good adhesion.

Based on the contribution of the substrate in the deposition process, substrate surface treatments are categorized into three categories, namely: surface texture, substrate temperature and surface roughening. Polishing for metals or grinding or grit blasting and /or sandblasting are the major surface preparation. In CGDS, substrate roughness prorogued the general on the effects it has on the bonding strength and adhesion. Grit blasting or sandblasting is more preferred during typical surface preparation to remove from metal surfaces the oxides. Surface texturing is a special novelty from the laser technology for surface preparation to provide substrate surface with micro holes a high-fidelity pattern which contains particles when impacting the substrate surface preceding deposition. The Bonding strength is improved using this method by creating a regular bond between particle/substrate interfaces. Substrate heating is another surface treatment during deposition. The literature has revealed that adhesion can be promoted by substrate heating as a result of thermo-mechanical softening.

The efficiency of cold gas dynamic spraying applications depends solely on: (A). impact behaviour of process parameters during deposition as well as particle thermal kinetics; (B). deposition efficiency optimization; and (C) structural changes prediction that determine the deposit final properties, even though numerous benefits have been derived to date through experimental and numerical analysis of the CGDS process. In a nutshell, through the exponential growth of this new emerging technology, this decade will see a drastical improvement of the technology through the development of further coatings for specific applications.

References

1. E. Irissou, J.-G. Legoux, A.N. Ryabinin, B. Jodoin, C. Moreau, Review on cold spraying processes and technology: Part I – Intellectual property, J. Therm. Spray Technol. **17** (2008) 495–516
2. R.N. Raoelison, Y. Xie, T. Sapanathan, M.P. Planche, R. Kromer, S. Costil et al., Cold gas dynamic spray technology: a comprehensive review of processing conditions for various technological developments till to date, Addit. Manuf. **19** (2018) 134–159
3. H. Singh, T.S. Sidhu, S.B.S. Kalsi, Cold spraying technology: future of coating deposition processes, Frat. Ed. Integrita Strutt. **22** (2012) 69–84
4. D.K. Christoulis, M. Jeandin, E. Irissou, J. Legoux, W. Knapp, Laser-Assisted Cold spraying (LACS) (2012) DOI: 10.5772/36104
5. A. Moridi, S.M. Hassani-Gangaraj, M. Guagliano, M. Dao, Cold spraying coating: review of material systems and future perspectives, Surf. Eng. **30** (2014) 369–395
6. T. Marrocco, D.G. McCartney, P.H. Shipway, A.J. Sturgeon, Production of titanium deposits by cold-gas dynamic spray: numerical modeling and experimental characterization, J. Therm. Spray Technol. **15** (2006) 263–272
7. D. MacDonald, R. Fernández, F. Delloro, B. Jodoin, Cold spraying of armstrong process titanium powder for additive manufacturing, J. Therm. Spray Technol. **26** (2017) 598–609

8. T.H.V. Steenkiste, J.R. Smith, R.E. Teets, Aluminum coatings via kinetic spray with relatively large powder particles, Surf. Coatings Technol. **154** (2002) 237–252
9. M. Grujicic, C.L. Zhao, C. Tong, W.S. DeRosset, D. Helfritch, Analysis of the impact velocity of powder particles in the cold-gas dynamic-spraying processes, Mater. Sci. Eng. A **368** (2004) 222–230
10. H. Assadi, F. Gartner, T. Stoltenhoff, H. Kreye, Bonding mechanism in cold gas spraying, Acta Mater. **6454** (2003) 4379–4394
11. R. Lupoi, W. O'Neill, Powder stream characteristics in cold spraying nozzles, Surf. Coatings Technol. **206** (2011) 1069–1076
12. R. Lupoi, W. O'Neill, Deposition of metallic coatings on polymer surfaces using cold spraying, Surf. Coatings Technol. **205** (2010) 2167–2173
13. J. Villafuerte, Current and future applications of cold spraying technology, Met. Finish. **108** (2010) 37–39
14. W.J. Marple, The Cold Gas-Dynamic Spray and Characterization of Microcrystalline and Nanocrystalline Copper Alloys. United States Naval Academy, Naval Postgraduate School, 2012
15. J.R. Davis, Handbook of thermal spray technology, ASM International, Materials Park, OH, USA, 2004
16. F.J. Hermanek, Thermal spray terminology and company origins, 1st edn. ASM International, Materials Park, OH, USA, 2001
17. R. Ghelichi, M. Guagliano, Coating by the Cold spraying processes: a state of the art. Frat Ed Integrità Strutt Ed Integrità Strutt **3** (2009) 30–44
18. S.E. Tinashe, Conceptual Design of a Low Pressure Cold Gas Dynamic Spray (LPCGDS) System, University of the Witwatersrand (2010)
19. H. Singh, T.S. Sidhu, S.B.S. Kalsi, J. Karthikeyan, Development of cold spraying from innovation to emerging future coating technology, J. Br. Soc. Mech. Sci. Eng. **35** (2013) 231–245
20. S. Yin, P. Cavaliere, B. Aldwell, R. Jenkins, H. Liao, W. Li et al., Cold spraying additive manufacturing and repair: fundamentals and applications, Addit. Manuf. **21** (2018) 628–650
21. D.G. McCartney, H. Tabbara, S. Gu, P.H. Shipway, T.S. Price, Study on process optimization of cold gas spraying, J. Therm. Spray Technol. **20** (2010) 608–620
22. Y.K. Han, N. Birbilis, K. Spencer, M. Zhang, B.C. Muddle, Investigation of Cu coatings deposited by kinetic metallization, Mater. Charact. **61** (2010) 1167–1186
23. F. Robitaille, M. Yandouzi, S. Hind, B. Jodoin, Metallic coating of aerospace carbon/epoxy composites by the pulsed gas dynamic spraying process, Surf. Coatings Technol. **203** (2009) 2954–2960
24. M. Yandouzi, P. Richer, B. Jodoin, SiC particulate reinforced Al − 12Si alloy composite coatings produced by the pulsed gas dynamic spraying processes: microstructure and properties, Surf. Coat. Technol. **203** (2009) 3260–3270
25. M. Yandouzi, H. Bu, M. Brochu, B. Jodoin, Nanostructured Al-based metal matrix composite coating production by pulsed gas dynamic spraying process, J. Therm. Spray Technol. **21** (2012) 609–619
26. M. Winnicki, A. Ma, G. Dudzik, M. Rutkowska-gorczyca, M. Marciniak, K. Abramski, Numerical and experimental analysis of copper particles velocity in low-pressure cold spraying process, Surf. Coat. Technol. **268** (2015) 230–240
27. D. Hanft, P. Glosse, S. Denneler, T. Berthold, M. Oomen, S.K. Id et al., The aerosol deposition method: a modified aerosol generation unit to improve coating quality. Material (Basel) **11** (2018) 1–11
28. H. Ashizawa, M. Kiyohara, Plasma exposure behavior of yttrium oxide film formed by aerosol deposition method, IEEE Trans. Semicond. Manuf. **30** (2017) 357–361
29. A. Concustell, J. Henao, S. Dosta, N. Cinca, I.G. Cano, J.M. Guilemany, On the formation of metallic glass coatings by means of Cold Gas Spray technology, J. Alloys Compd. **651** (2015) 764–772
30. D.P. Eason, A structure property processing comparison of cold rolled PM copper and cold gas dynamically sprayed copper, J. Powder Metall. Min. **01** (2012) 1–5
31. M.R. Rokni, C.A. Widener, G.A. Crawford, M.K. West, An investigation into microstructure and mechanical properties of cold sprayed 7075 Al deposition, Mater. Sci. Eng. A **625** (2015) 19–27
32. Y. Zou, W. Qin, E. Irissou, J.-G. Legoux, S. Yue, J.A. Szpunar, Dynamic recrystallization in the particle/particle interfacial region of cold-sprayed nickel coating: electron backscatter diffraction characterization, Scr. Mater. **61** (2009) 899–902
33. D. Rafaja, T. Schucknecht, V. Klemm, A. Paul, H. Berek, Microstructural characterisation of titanium coatings deposited using cold gas spraying on Al_2O_3 substrates, Surf. Coatings Technol. **203** (2009) 3206–3213
34. M.R. Rokni, C.A. Widener, G.A. Crawford, M.K. West, An investigation into microstructure and mechanical properties of cold sprayed 7075 Al deposition, Mater. Sci. Eng. A **625** (2015) 19–27
35. D. Giraud, Étude des composantes mécanique et métallurgique dans la liaison revêtement-substrat obtenue par projection dynamique par gaz froid pour les systèmes "Aluminium / Polyamide6, 6" et "Titane / TA6V" To cite this version: HAL Id: pastel-01073679 l ' É 2014
36. M. Grujicic, J.R. Saylor, D.E. Beasley, W.S. DeRosset, D. Helfritch, Computational analysis of the interfacial bonding between feed-powder particles and the substrate in the cold-gas dynamic-spraying processes, Appl. Surf. Sci. **219** (2003) 211–227
37. X.L. Zhou, A.F. Chen, J.C. Liu, X.K. Wu, J.S. Zhang, Preparation of metallic coatings on polymer matrix composites by cold spraying, Surf. Coatings Technol. **206** (2011) 132–136
38. V.K. Champagne, D. Helfritch, P. Leyman, S. Grendahl, B. Klotz, Interface material mixing formed by the deposition of copper on aluminum by means of the cold spraying processes, J. Therm. Spray Technol. **14** (2005) 330–334
39. K.H. Ko, J.O. Choi, H. Lee, Intermixing and interfacial morphology of cold-sprayed Al coatings on steel, Mater. Lett. **136** (2014) 45–47
40. A. Ganesan, M. Yamada, M. Fukumoto, Cold spraying coating deposition mechanism on the thermoplastic and thermosetting polymer substrates, J. Therm. Spray Technol. **22** (2013) 1275–1282
41. D. Seo, M. Sayar, K. Ogawa, SiO_2 and $MoSi_2$ formation on Inconel 625 surface via SiC coating deposited by cold spraying, Surf. Coatings Technol. **206** (2012) 2851–2858
42. T. Hussain, D.G. McCartney, P.H. Shipway, Bonding between aluminium and copper in cold spraying: story of asymmetry, Mater. Sci. Technol. **28** (2012) 1371–1378

43. D.-Y. Kim, J.-J. Park, J.-G. Lee, D. Kim, S.J. Tark, S. Ahn et al., Cold spraying deposition of copper electrodes on silicon and glass substrates, J. Therm. Spray Technol. **22** (2013) 1092–1102
44. H.Y. Lee, Y.H. Yu, Y.C. Lee, Y.P. Hong, K.H. Ko, Interfacial studies between cold-sprayed WO3, Y2O3 films and Si substrate, Appl. Surf. Sci. **227** (2004) 244–249
45. I. Burlacov, J. Jirkovský, L. Kavan, R. Ballhorn, R.B. Heimann, Cold gas dynamic spraying (CGDS) of TiO_2 (anatase) powders onto poly(sulfone) substrates: microstructural characterisation and photocatalytic efficiency, J. Photochem. Photobiol. A: Chem. **187** (2007) 285–292
46. A. Ganesan, J. Affi, M. Yamada, M. Fukumoto, Bonding behavior studies of cold sprayed copper coating on the PVC polymer substrate, Surf. Coatings Technol. **207** (2012) 262–269
47. D. Zhang, P.H. Shipway, D.G. McCartney, Cold gas dynamic spraying of aluminum: the role of substrate characteristics in deposit formation, J. Therm. Spray Technol. **14** (2005) 109–116
48. P.C. King, S. Zahiri, M. Jahedi, J. Friend, Aluminium coating of lead zirconate titanate—a study of cold spraying variables, Surf. Coatings Technol. **205** (2010) 2016–2222
49. P.C. King, A.J. Poole, S. Horne, R. de Nys, S. Gulizia, M.Z. Jahedi, Embedment of copper particles into polymers by cold spraying, Surf. Coatings Technol. **216** (2013) 60–67
50. A.S. Alhulaifi, G.A. Buck, W.J. Arbegast, Numerical and experimental investigation of cold spraying gas dynamic effects for polymer coating, J. Therm. Spray Technol. **21** (2012) 852–862
51. Y. Xu, I.M. Hutchings, Cold spraying deposition of thermoplastic powder, Surf. Coatings Technol. **201** (2006) 3044–3050
52. L. Zhu, T.-C. Jen, Y.-T. Pan, H.-S. Chen, Particle bonding mechanism in cold gas dynamic spray: a three-dimensional approach, J. Therm. Spray Technol. **26** (2017) 1859–1873
53. Y. Kim, S. Yang, J.-W. Lee, J.-O. Choi, S.-H. Ahn, C.S. Lee, Photovoltaic characteristics of a Dye-Sensitized Solar Cell (DSSC) fabricated by a Nano-Particle Deposition System (NPDS), Mater. Trans. **54** (2013) 2064–2068
54. D.-M. Chun, S.-H. Ahn, Deposition mechanism of dry sprayed ceramic particles at room temperature using a nano-particle deposition system, Acta Mater. **59** (2011) 2693–2703
55. H.Y. Lee, Y.H. Yu, Y.C. Lee, Y.P. Hong, K.H. Ko, Thin film coatings of WO_3 by cold gas dynamic spray: a technical note, J. Therm. Spray Technol. **14** (2005) 183–186
56. S.-Q. Fan, C.-J. Li, G.-J. Yang, L.-Z. Zhang, J.-C. Gao, Y.-X. Xi, Fabrication of nano-TiO_2 coating for dye-sensitized solar cell by vacuum cold spraying at room temperature, J. Therm. Spray Technol. **16** (2007) 893–897
57. M. Yamada, H. Isago, H. Nakano, M. Fukumoto, Cold spraying of TiO_2 photocatalyst coating with nitrogen process gas, J. Therm. Spray Technol. **19** (2010) 1218–1223
58. S.-Q. Fan, G.-J. Yang, C.-J. Li, G.-J. Liu, C.-X. Li, L.-Z. Zhang, Characterization of microstructure of Nano-TiO2 coating deposited by vacuum cold spraying, J. Therm. Spray Technol. **15** (2006) 513–517
59. R.N. Raoelison, C. Verdy, H. Liao, Cold gas dynamic spray additive manufacturing today: Deposit possibilities, technological solutions and viable applications, Mater. Des. **133** (2017) 266–287
60. H. Assadi, T. Schmidt, H. Richter, J.-O. Kliemann, K. Binder, F. Gärtner et al., On parameter selection in cold spraying, J. Therm. Spray Technol. **20** (2011) 1161–1176
61. M. Fukumoto, H. Terada, M. Mashiko, K. Sato, M. Yamada, E. Yamaguchi, Deposition of copper fine particle by cold spraying processes, Mater. Trans. **50** (2009) 1482–1488
62. G.-J. Yang, C.-J. Li, S.-Q. Fan, Y.-Y. Wang, C.-X. Li, Influence of annealing on photocatalytic performance and adhesion of vacuum cold-sprayed nanostructured TiO_2 coating, J. Therm. Spray Technol. **16** (2007) 873–880
63. Y.-Y. Wang, L. Yi, C.-X. Li, G.-J. Yang, Y. Liu, C.-J. Li et al., Electrical and mechanical properties of nano-structured TiN coatings deposited by vacuum cold spraying coating microstructure control view project the cracking mechanism of thermally sprayed coatings view project electrical and mechanical properties of nano-, Vaccum **86** (2012) 953–959
64. D.-M. Chun, C.-S. Kim, J.-O. Choi, G.-Y. Lee, C.S. Lee, S.-H. Ahn, Multilayer deposition of ceramic and metal at room temperature using nanoparticle deposition system (NPDS) and planarization process, Int. J. Adv. Manuf. Technol. **72** (2014) 41–46
65. D.M. Chun, M.H. Kim, J.C. Lee, S.H. Ahn, TiO_2 coating on metal and polymer substrates by nano-particle deposition system (NPDS), CIRP Ann. **57** (2008) 551–554
66. D.-M. Chun, J.-O. Choi, C.S. Lee, I. Kanno, H. Kotera, S.-H. Ahn, Nano-particle deposition system (NPDS): low energy solvent-free dry spraying processes for direct patterning of metals and ceramics at room temperature, Int. J. Precis. Eng. Manuf. **13** (2012) 1107–1112
67. S.-Q. Fan, C.-J. Li, G.-J. Yang, L.-Z. Zhang, J.-C. Gao, Y.-X. Xi, Fabrication of nano-TiO 2 coating for dye-sensitized solar cell by vacuum cold spraying at room temperature, J. Therm. Spray Technol. **16** (2007) 892–897
68. R. Kromer, R.N. Raoelison, C. Langlade, Y. Xie, M.P. Planche, T. Sapanathan et al., Cold gas dynamic spray technology: a comprehensive review of processing conditions for various technological developments till to date, Addit. Manuf. **19** (2017) 134–159
69. J. Karthikeyan, Cold spraying Technology: International Status and USA Efforts (2004) 1–14
70. C.-J. Li, H.-T. Wang, Q. Zhang, G.-J. Yang, W.-Y. Li, H.L. Liao, Influence of spray materials and their surface oxidation on the critical velocity in cold spraying, J. Therm. Spray Technol. **19** (2010) 95–101
71. C.-J. Li, W.-Y. Li, Deposition characteristics of titanium coating in cold spraying, Surf. Coatings Technol. **167** (2003) 278–283
72. C.-J. Li, W.-Y. Li, Y.-Y. Wang, G.-J. Yang, H. Fukanuma, A theoretical model for prediction of deposition efficiency in cold spraying, Thin Solid Films **489** (2005) 79–85
73. C.-J. Li, W.-Y. Li, H. Liao, Examination of the critical velocity for deposition of particles in cold spraying, J. Therm. Spray Technol. **15** (2006) 212–222
74. J.-G. Legoux, E. Irissou, S. Desaulniers, J. Bobyn, B. Harvey, W. Wong, E. Gagnon, S. Yue, Characterization and performance evaluation of a helium recovery system designed for cold spraying, NRC Publ Arch (NPArC) 2010, 1–22
75. C.J. Sutcliffe, A. Papworth, C. Gallagher, P. Fox, R.H. Morgan, W. O'Neill et al., Cold gas dynamic manufacturing – a new approach to near-net shape metal component fabrication, Mater. Res. Soc. Proc. **758** (2003) 73–84

76. W. Wong, E. Irissou, A.N. Ryabinin, J. Legoux, S. Yue, Influence of helium and nitrogen gases on the properties of cold gas dynamic sprayed pure titanium coatings, J. Therm. Spray Technol. **20** (2011) 213–226
77. S. Yin, X. Suo, H. Liao, Z. Guo, X. Wang, Significant influence of carrier gas temperature during the cold spraying processes, Surf. Eng. **30** (2014) 443–450
78. S. Yin, Q. Liu, H. Liao, X. Wang, Effect of injection pressure on particle acceleration, dispersion and deposition in cold spraying, Comput. Mater. Sci. **90** (2014) 7–15
79. S. Yin, Y. Xie, X. Suo, H. Liao, X. Wang, Interfacial bonding features of Ni coating on Al substrate with different surface pretreatments in cold spraying, Mater. Lett. **138** (2015) 143–147
80. T. Hussain, D.G. McCartney, P.H. Shipway, Impact phenomena in cold-spraying of titanium onto various ferrous alloys, Surf. Coatings Technol. **205** (2011) 5021–5027
81. J. Wu, J. Yang, H. Fang, S. Yoon, C. Lee, The bond strength of Al-Si coating on mild steel by kinetic spraying deposition, Appl. Surf. Sci. **252** (2006) 7809–7814
82. P. Richer, B. Jodoin, L. Ajdelsztajn, E.J. Lavernia, Substrate roughness and thickness effects on cold spraying nanocrystalline Al-Mg coatings, J. Therm. Spray Technol. **15** (2006) 246–254
83. C.R. May, C. May, S. Marx, A. Paul, Cold spraying coatings on hard surfaces other commercial applications, n.d.
84. K.-R. Ernst, J. Braeutigam, F. Gaertner, T. Klassen, Effect of substrate temperature on cold-gas-sprayed coatings on ceramic substrates, J. Therm. Spray Technol. **22** (2013) 422–432
85. R. Kromer, S. Costil, J. Cormier, L. Berthe, P. Peyre, D. Courapied, Laser patterning pretreatment before thermal spraying: a technique to adapt and control the surface topography to thermomechanical loading and materials, J. Therm. Spray Technol. **25** (2016) 401–410
86. R. Kromer, S. Costil, C. Verdy, S. Gojon, H. Liao, Laser surface texturing to enhance adhesion bond strength of spray coatings – cold spraying, wire-arc spraying, and atmospheric plasma spraying, Surf. Coatings Technol. **352** (2018) 642–653
87. M. Yu, W.-Y. Li, F.F. Wang, X.K. Suo, H.L. Liao, Effect of particle and substrate preheating on particle deformation behavior in cold spraying, Surf. Coatings Technol. **220** (2013) 174–178
88. S. Yin, X. Suo, Z. Guo, H. Liao, X. Wang, Deposition features of cold sprayed copper particles on preheated substrate, Surf. Coatings Technol. **268** (2015) 252–256
89. Y. Xie, M.-P. Planche, R. Raoelison, H. Liao, X. Suo, P. Hervé, Effect of substrate preheating on adhesive strength of SS 316L cold spraying coatings, J. Therm. Spray Technol. **25** (2016) 123–130
90. X.K. Suo, M. Yu, W.Y. Li, M.P. Planche, H.L. Liao, Effect of substrate preheating on bonding strength of cold-sprayed Mg coatings, J. Therm. Spray Technol. **21** (2012) 1091–1098
91. S. Yin, X. Suo, Y. Xie, W. Li, R. Lupoi, H. Liao, Effect of substrate temperature on interfacial bonding for cold spraying of Ni onto Cu, J. Mater. Sci. **50** (2015) 7448–7457
92. N.M. Chavan, M. Ramakrishna, P.S. Phani, D.S. Rao, G. Sundararajan, The influence of process parameters and heat treatment on the properties of cold sprayed silver coatings, Surf. Coatings Technol. **205** (2011) 4798–4807
93. R. Morgan, P. Fox, J. Pattison, C. Sutcliffe, W. O'Neill, Analysis of cold gas dynamically sprayed aluminium deposits, Mater. Lett. **58** (2004) 1317–1320
94. Q. Wang, N. Birbilis, M.-X. Zhang, Interfacial structure between particles in an aluminum deposit produced by cold spraying, Mater. Lett. **65** (2011) 1576–1578
95. C.W. Ziemian, M.M. Sharma, B.D. Bouffard, T. Nissley, T. J. Eden, Effect of substrate surface roughening and cold spraying coating on the fatigue life of AA2024 specimens, Mater. Des. **54** (2014) 212–221
96. K. Balani, T. Laha, A. Agarwal, J. Karthikeyan, N. Munroe, Effect of carrier gases on microstructural and electrochemical behavior of cold-sprayed 1100 aluminum coating, Surf. Coatings Technol. **195** (2005) 272–279
97. L. Ajdelsztajn, A. Zúñiga, B. Jodoin, E.J. Lavernia, Cold gas dynamic spraying of a high temperature Al alloy, Surf. Coatings Technol. **201** (2006) 2109–2116
98. B. Jodoin, L. Ajdelsztajn, E. Sansoucy, A. Zúñiga, P. Richer, E.J. Lavernia, Effect of particle size, morphology, and hardness on cold gas dynamic sprayed aluminum alloy coatings, Surf. Coatings Technol. **201** (2006) 3422–3429
99. R. Ghelichi, S. Bagherifard, D. Mac Donald, M. Brochu, H. Jahed, B. Jodoin et al., Fatigue strength of Al alloy cold sprayed with nanocrystalline powders, Int. J. Fatigue **65** (2014) 51–57
100. K. Spencer, M.-X. Zhang, Heat treatment of cold spraying coatings to form protective intermetallic layers, Scr. Mater. **61** (2009) 44–47
101. Y. Tao, T. Xiong, C. Sun, L. Kong, X. Cui, T. Li et al., Microstructure and corrosion performance of a cold sprayed aluminium coating on AZ91D magnesium alloy, Corros. Sci. **52** (2010) 3191–3197
102. H. Bu, M. Yandouzi, C. Lu, B. Jodoin, Effect of heat treatment on the intermetallic layer of cold sprayed aluminum coatings on magnesium alloy, Surf. Coatings Technol. **205** (2011) 4665–4671
103. A.P. Alkhimov, N.I. Nesterovich, A.N. Papyrin, Experimental investigation of supersonic two-phase flow over bodies, J. Appl. Mech. Tech. Phys. **23** (1982) 219–226
104. H. Lee, H. Shin, S. Lee, K. Ko, Effect of gas pressure on Al coatings by cold gas dynamic spray, Mater. Lett. **62** (2008) 1579–1581
105. T. Hussain, Cold spraying of titanium: a review of bonding mechanisms, microstructure and properties, Key Eng. Mater. Online **533** (2013) 53–90
106. S. Yin, X. Wang, X. Suo, H. Liao, Z. Guo, W. Li et al., Deposition behavior of thermally softened copper particles in cold spraying, Acta Mater. **61** (2013) 5105–5118
107. P.D. Eason, J.A. Fewkes, S.C. Kennett, T.J. Eden, K. Tello, M.J. Kaufman et al., On the characterization of bulk copper produced by cold gas dynamic spraying processesing in as fabricated and annealed conditions, Mater. Sci. Eng. A **528** (2011) 8174–8178
108. H.-J. Choi, M. Lee, J.Y. Lee, Application of a cold spraying technique to the fabrication of a copper canister for the geological disposal of CANDU spent fuels, Nucl. Eng. Des. **240** (2010) 2714–2720
109. M. Fukumoto, H. Terada, M. Mashiko, K. Sato, M. Yamada, E. Yamaguchi, Deposition of copper fine particle by cold spraying processes, Mater. Trans. **50** (2009) 1482–1488

110. M. Fukumoto, H. Wada, K. Tanabe, M. Yamada, E. Yamaguchi, A. Niwa et al. Effect of Substrate temperature on deposition behavior of copper particles on substrate surfaces in the cold spraying processes, J. Therm. Spray Technol. **16** (2007) 643–650
111. P. Poza, C.J. Múnez, M.A. Garrido-Maneiro, S. Vezzù, S. Rech, A. Trentin, Mechanical properties of Inconel 625 cold-sprayed coatings after laser remelting. Depth sensing indentation analysis, Surf. Coatings Technol. **243** (2014) 51–57
112. D. Levasseur, S. Yue, M. Brochu, Pressureless sintering of cold sprayed Inconel 718 deposit, Mater. Sci. Eng. A **556** (2012) 343–350
113. X. Meng, J. Zhang, J. Zhao, Y. Liang, Y. Zhang, Influence of gas temperature on microstructure and properties of cold spraying 304SS coating, J. Mater. Sci. Technol. **27** (2011) 809–815
114. A. Sova, S. Grigoriev, A. Okunkova, I. Smurov, Cold spraying deposition of 316L stainless steel coatings on aluminium surface with following laser post-treatment, Surf. Coatings Technol. **235** (2013) 283–289
115. M. Villa, S. Dosta, J.M. Guilemany, Optimization of 316L stainless steel coatings on light alloys using Cold Gas Spray, Surf. Coatings Technol. **235** (2013) 220–225
116. G. Bolelli, B. Bonferroni, H. Koivuluoto, L. Lusvarghi, P. Vuoristo, Depth-sensing indentation for assessing the mechanical properties of cold-sprayed Ta, Surf. Coatings Technol. **205** (2010) 2209–2217
117. R.S. Lima, A. Kucuk, C.C. Berndt, J. Karthikeyan, C.M. Kay, J. Lindemann, Deposition efficiency, mechanical properties and coating roughness in cold-sprayed titanium, J. Mater. Sci. Lett. **21** (2002) 1687–1689
118. C.K.S. Moy, J. Cairney, G. Ranzi, M. Jahedi, S.P. Ringer, Investigating the microstructure and composition of cold gas-dynamic spray (CGDS) Ti powder deposited on Al 6063 substrate, Surf. Coatings Technol. **204** (2010) 3739–3749
119. H.-R. Wang, W.-Y. Li, L. Ma, J. Wang, Q. Wang, Corrosion behavior of cold sprayed titanium protective coating on 1Cr13 substrate in seawater, Surf. Coatings Technol. **201** (2007) 5203–5206
120. S.H. Zahiri, C.I. Antonio, M. Jahedi, Elimination of porosity in directly fabricated titanium via cold gas dynamic spraying, J. Mater. Process. Technol. **209** (2009) 922–929
121. J. Cizek, O. Kovarik, J. Siegl, K.A. Khor, I. Dlouhy, Influence of plasma and cold spraying deposited Ti Layers on high-cycle fatigue properties of Ti6Al4V substrates, Surf. Coatings Technol. **217** (2013) 23–33
122. F. Robitaille, M. Yandouzi, S. Hind, B. Jodoin, Metallic coating of aerospace carbon/epoxy composites by the pulsed gas dynamic spraying process, Surf. Coatings Technol. **203** (2009) 2954–2960
123. W.-Y. Li, C.-J. Li, G.-J. Yang, Effect of impact-induced melting on interface microstructure and bonding of cold-sprayed zinc coating, Appl. Surf. Sci. **257** (2010) 1516–1523
124. W.-Y. Li, C. Zhang, X.P. Guo, G. Zhang, H.L. Liao, C.-J. Li, et al. Effect of standoff distance on coating deposition characteristics in cold spraying, Mater Des. **29** (2008) 297–304
125. J.G. Legoux, E. Irissou, C. Moreau, Effect of substrate temperature on the formation mechanism of cold-sprayed aluminum, zinc and tin coatings, J. Therm. Spray Technol. **16** (2007) 619–626
126. Z.B. Zhao, B.A. Gillispie, J.R. Smith, Coating deposition by the kinetic spraying processes, Surf. Coatings Technol. **200** (2006) 4746–4754
127. T. Van, H. Steenkiste, J.R. Smith, R.E. Teets, J.J. Moleski, D.W. Gorkiewicz, R.P. Tison et al., Kinetic spray coatings, Surf. Coatings Technol. **111** (1999) 62–71
128. F. Raletz, M. Vardelle, G. Ezo'o, Critical particle velocity under cold spraying conditions, Surf. Coatings Technol. **201** (2006) 1942–1947
129. C.-J. Li, W.-Y. Li, Y.-Y. Wang, Effect of Spray Angle on Deposition Characteristics in Cold spraying, ASM International, Therm. Spray, Ohio USA, **2003**, pp. 91–96
130. H. Fukanuma, N. Ohno, B. Sun, R. Huang, In-flight particle velocity measurements with DPV-2000 in cold spraying, Surf. Coatings Technol. **201** (2006) 1935–1941.
131. W.-Y. Li, C. Zhang, H.-T. Wang, X.P. Guo, H.L. Liao, C.-J. Li et al., Significant influences of metal reactivity and oxide films at particle surfaces on coating microstructure in cold spraying, Appl. Surf. Sci. **253** (2007) 3557–3562
132. M. Yandouzi, P. Richer, B. Jodoin, SiC particulate reinforced Al-12Si alloy composite coatings produced by the pulsed gas dynamic spraying processes: microstructure and properties, Surf. Coatings Technol. **203** (2009) 3260–3270
133. X.-J. Ning, J.-H. Kim, H.-J. Kim, C. Lee, Characteristics and heat treatment of cold-sprayed Al–Sn binary alloy coatings, Appl. Surf. Sci. **255** (2009) 3933–3939
134. X.-J. Ning, J.-H. Jang, H.-J. Kim, C.-J. Li, C. Lee, Cold spraying of Al-Sn binary alloy: Coating characteristics and particle bonding features, Surf. Coatings Technol. **202** (2008) 1681–1687
135. E. Sansoucy, G.E. Kim, A.L. Moran, B. Jodoin, Mechanical characteristics of Al-Co-Ce coatings produced by the cold spraying processes, J. Therm. Spray Technol. **16** (2007) 651–660
136. P. Coddet, C. Verdy, C. Coddet, F. Lecouturier, F. Debray, Mechanical properties of Cold spraying deposited NARloy-Z copper alloy, Surf. Coatings Technol. **232** (2013) 652–657
137. S.V. Raj, C. Barrett, J. Karthikeyan, R. Garlick, Comparison of the cyclic oxidation behavior of cold sprayed CuCrAl-coated and uncoated GRCop-84 substrates for space launch vehicles, Surf. Coatings Technol. **201** (2007) 7222–7234
138. W.-Y. Li, C.-J. Li, H. Liao, C. Coddet, Effect of heat treatment on the microstructure and microhardness of cold-sprayed tin bronze coating, Appl. Surf. Sci. **253** (2007) 5967–5971
139. X. Guo, G. Zhang, W.-Y. Li, L. Dembinski, Y. Gao, H. Liao et al., Microstructure, microhardness and dry friction behavior of cold-sprayed tin bronze coatings, Appl. Surf. Sci. **254** (2007) 1482–1488
140. N. Cinca, E. López, S. Dosta, J.M. Guilemany, Study of stellite-6 deposition by cold gas spraying, Surf. Coatings Technol. **232** (2013) 891–898
141. N. Cinca, J.M. Guilemany, Structural and properties characterization of stellite coatings obtained by cold gas spraying, Surf. Coatings Technol. **220** (2013) 90–97
142. S. Rech, A. Surpi, S. Vezzù, A. Patelli, A. Trentin, J. Glor, et al., Cold-spray deposition of Ti2AlC coatings. Vacuum **94** (2013) 69–73
143. D.-M. Chun, J.-O. Choi, C.S. Lee, S.-H. Ahn, Effect of stand-off distance for cold gas spraying of fine ceramic particles (<5 μm) under low vacuum and room temperature using nano-particle deposition system (NPDS), Surf. Coatings Technol. **206** (2012) 2125–2132

144. P. Richer, M. Yandouzi, L. Beauvais, B. Jodoin, Oxidation behaviour of CoNiCrAlY bond coats produced by plasma, HVOF and cold gas dynamic spraying, Surf. Coatings Technol. **204** (2010) 3962–3974
145. A. Bonadei, T. Marrocco, Cold sprayed MCrAlY + X coating for gas turbine blades and vanes, Surf. Coatings Technol. **242** (2014) 200–206
146. G.-C. Ji, H.-T. Wang, X. Chen, X.-B. Bai, Z.-X. Dong, F-G. Yang, Characterization of cold-sprayed multimodal WC-12Co coating, Surf. Coatings Technol. **235** (2013) 536–543
147. H.-J. Kim, C.-H. Lee, S-Y. Hwang, Fabrication of WC-Co coatings by cold spraying deposition, Surf. Coatings Technol. **191** (2005) 335–340
148. A.S.M. Ang, C.C. Berndt, P. Cheang, Deposition effects of WC particle size on cold sprayed WC-Co coatings, Surf. Coatings Technol. **205** (2011) 3260–3267
149. S. Dosta, M. Couto, J.M. Guilemany, Cold spraying deposition of a WC-25Co cermet onto Al7075-T6 and carbon steel substrates, Acta Mater. **61** (2013) 643–652
150. M. Yandouzi, E. Sansoucy, L. Ajdelsztajn, B. Jodoin, WC-based cermet coatings produced by cold gas dynamic and pulsed gas dynamic spraying processes, Surf. Coatings Technol. **202** (2007) 382–390
151. W.-Y. Li, C.-J. Li, Optimal design of a novel cold spraying gun nozzle at a limited space, J ThermSpray Technol. **14** (2005) 391–396
152. J. Karthikeyan, Development of oxidation resistant coatings on GRCop-84 substrates by cold spraying processes. NASA/CR 2007, 214706
153. V.K. Champagne, P.F. Leyman, D. Helfritch, Magnesium repair by cold spraying, Plant. Surf. Finish. **95** (2008) 34
154. B. DeForce, T. Eden, J. Potter, V. Champagne, P. Leyman, D. Helfritch, Application of aluminum coatings for the corrosion protection of magnesium by cold spraying, TRI Serv. Corros. (2007) 1–16
155. J. Villafuerte, Current and future applications of cold spraying technology, Met. Finish. **108** (2010) 37–39
156. A. Shkodkin, A. Kashirin, O. Klyuev, T. Buzdygar, Peculiarities of Gas Dynamic Spray Applications in Russia, 2010.
157. A. Sova, S. Grigoriev, A. Okunkova, I. Smurov, Potential of cold gas dynamic spray as additive manufacturing technology, Int. J. Adv. Manuf. Technol. **69** (2013) 2269–2278
158. S. Yoon, H. Kim, C. Lee, Fabrication of automotive heat exchanger using kinetic spraying process, Surf. Coat. Technol. **201** (2007) 9524–9932
159. A. Choudhuri, P.S. Mohanty, J. Karthikeyan, Bioceramic composite coatings by cold spraying technology, Addit. Manuf. Process (2009)
160. K. Balani, A. Agarwal, S. Seal, J. Karthikeyan, Transmission electron microscopy of cold sprayed 1100 aluminum coating, Scr. Mater. **53** (2005) 845–850
161. V.K. Champagne, The repair of magnesium rotorcraft components by cold spraying, J. Fail. Anal. Prev. **8** (2008) 164–175
162. H. Assadi, H. Kreye, F. Gärtner, T. Klassen, Cold spraying − a materials perspective, Acta Mater. **116** (2016) 382–407

Cite this article as: Sunday Temitope Oyinbo, Tien-Chien Jen, A comparative review on cold gas dynamic spraying processes and technologies, Manufacturing Rev. **6**, 25 (2019)